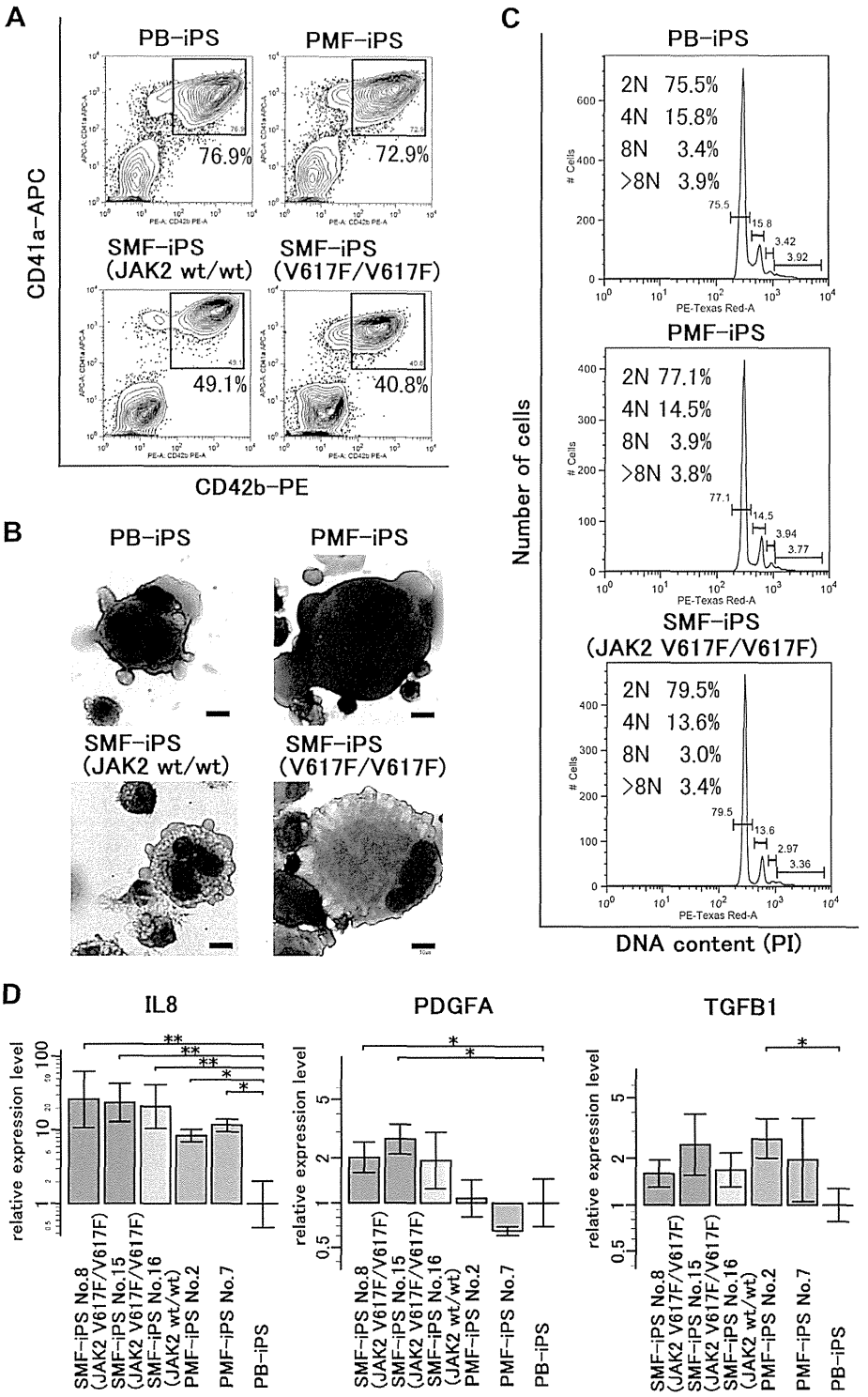

Figure 5. (**A**) Surface markers of myelofibrosis patient-derived induced pluripotent stem cells (MF-iPS)-derived megakaryocytes. (**B**) Morphology of megakaryocytes derived from MF-iPS. Wright–Giemsa staining. Original magnification: ×400. Black bars = 10 μm. (**C**) Ploidy analysis of sorted $CD41a^{+}42b^{+}$ megakaryocytes derived from MF-iPS. (**D**) Cytokine expression levels measured by real-time reverse transcription polymerase chain reaction assay. Error bars represent standard deviations (n = 3). BFU = burst forming units. $*p < 0.05$, $**p < 0.01$.

lobulated nuclei similar to those derived from normal iPS (Fig. 5B). DNA ploidy levels of megakaryocytes derived from MF-iPS were mostly not high (2N or 4N), but the fractions of polyploid cells (8N or more) were similar to those of normal iPS (Fig. 5C).

Expression of the genes encoding cytokines in MF-iPS-derived megakaryocytes

After obtaining megakaryocytes from MF-iPS, we analyzed the expression levels of the genes encoding cytokines by real-time reverse transcription PCR. As a result, in PMF-iPS- and SMF-iPS-derived megakaryocytes, IL-8 mRNA was largely increased, compared with the values in normal iPS-derived megakaryocytes (Fig. 5D). On the other hand, the mRNA levels of PDGF-α were only slightly higher in SMF-iPS-derived megakaryocytes, and those of TGF-β1 were slightly higher in PMF-iPS-derived megakaryocytes, both compared with normal iPS-derived megakaryocytes (Fig. 5D).

Discussion

The reprogramming of acquired hematologic diseases has been reported in polycythemia vera and chronic myeloid leukemia [19,20]. Here we described the successful reprogramming of cells from patients with primary and secondary myelofibrosis. The pluripotency of established MF-iPS was confirmed through expression of pluripotency markers and in vivo differentiation by teratoma formation. To establish disease-specific iPS from acquired diseases, the disease cells have to be obtained from an appropriate disease lesion, and in most cases, the disease cells need to have a reprogramming efficiency almost comparable to that of normal cells, which are inevitably mixed into the primary samples. Actually, the reprogramming of disease cells is often less efficient or takes longer than that of normal counterparts [21]. In this study, however, we succeeded in establishing iPS simply using primary samples of high disease cell frequency, mostly based on the protocol for the establishment of normal iPS from hematopoietic cells [22]. The presence of the JAK2 V617F mutation in SMF-iPS and the 13q deletion in PMF-iPS clearly confirmed they were generated from disease cells. Moreover, the time needed for establishment was comparable to that for normal blood cells. These results indicate that the primary cells of myelofibrosis were equivalent to their normal counterparts with respect to priming for reprogramming.

As mentioned above, megakaryocytes are considered to be responsible for generating effectors of myelofibrotic transformation in myelofibrosis. Therefore, megakaryocytes derived from myelofibrosis clones should be valuable in investigations of this difficult disease. By co-culture with feeder cells, the MF-iPS we established could be re-differentiated into blood cells and into megakaryocytes. By using these re-differentiated cells, we found that expression levels of the IL-8 gene were largely increased in whole MF-iPS-derived megakaryocytes as compared with normal iPS-derived megakaryocytes. IL-8, which is a cytokine known to stimulate fibroblasts to produce collagen and extracellular matrix, is highly elevated in patients with myelofibrosis, especially in those with a poor prognosis [11,23]. Therefore, the crosstalk between myelofibrosis disease cells and components of the microenvironment such as fibroblasts via IL-8 may be an attractive therapeutic target of this complex disease.

On the other hand, TGF-β1 and PDGF-α have been also considered as cytokines deeply involved in the promotion of bone marrow fibrosis and angiogenesis [24,25]. Recent global expression analyses, however, did not find these cytokine genes to be significantly upregulated in patient cells [26]. Our results also failed to indicate significant differences in the transcription levels of these cytokine genes between normal iPS- and MF-iPS-derived megakaryocytes. One possible explanation is that the difference in cytokine production could be a result of post-transcriptional abnormalities, which are induced by some stimuli in the in vivo microenvironment. Another possibility is that epigenetic modification of the promoter of TGF-β1 and PDGF-α genes in iPS-derived megakaryocytes has not followed correctly that in physiologically differentiated megakaryocytes. Indeed, the phenotypes of myelofibrosis, for example, megakaryocytes with an aberrant nuclear/cytoplasmic ratio and hyperchromatic, bulbous, or irregularly folded nuclei under microscopy, have not been fully recapitulated in MF-iPS-derived megakaryocytes. Further investigation would establish methods for generating more suitable disease model megakaryocytes from iPS.

Collectively, we found in this study that re-differentiated hematopoietic cells derived from MF-iPS, especially megakaryocytes, can be an alternative source of myelofibrosis patient disease cells, which are often extremely difficult to harvest abundantly. They should be useful in further research on this disease.

Acknowledgments

We thank K. Tsuji for special advice with experience, and Y. Hokama and Y. Izawa for technical assistance with experiments. Thrombopoietin receptor agonists rHuMGDF and rHuEPO were a kind gift from Kyowa Hakko Kirin. This work was supported by a grant-in-aid from Core Research for Evolutional Science and Technology (CREST), Tokyo, Japan, and the Tokyo Biochemical Research Foundation, Tokyo, Japan.

Conflict of interest disclosure

No financial interest/relationships with financial interest relating to the topic of this article have been declared.

References

1. Takahashi K, Tanabe K, Ohnuki M, et al. Induction of pluripotent stem cells from adult human fibroblasts by defined factors. Cell. 2007;131:861–872.

2. Maury Y, Gauthier M, Peschanski M, Martinat C. Human pluripotent stem cells for disease modelling and drug screening. Bioessays. 2012;34:61–71.
3. Cervantes F, Dupriez B, Pereira A, et al. New prognostic scoring system for primary myelofibrosis based on a study of the International Working Group for Myelofibrosis Research and Treatment. Blood. 2009;113:2895–2901.
4. Verstovsek S, Mesa RA, Gotlib J, et al. A double-blind, placebo-controlled trial of ruxolitinib for myelofibrosis. N Engl J Med. 2012;366:799–807.
5. Guardiola P, Anderson JE, Bandini G, et al. Allogeneic stem cell transplantation for agnogenic myeloid metaplasia: A European Group for Blood and Marrow Transplantation, Societe Francaise de Greffe de Moelle, Gruppo Italiano per il Trapianto del Midollo Osseo, and Fred Hutchinson Cancer Research Center Collaborative Study. Blood. 1999;93:2831–2838.
6. Rondelli D, Barosi G, Bacigalupo A, et al. Allogeneic hematopoietic stem-cell transplantation with reduced-intensity conditioning in intermediate- or high-risk patients with myelofibrosis with myeloid metaplasia. Blood. 2005;105:4115–4119.
7. Kroger N, Zabelina T, Schieder H, et al. Pilot study of reduced-intensity conditioning followed by allogeneic stem cell transplantation from related and unrelated donors in patients with myelofibrosis. Br J Haematol. 2005;128:690–697.
8. Merup M, Lazarevic V, Nahi H, et al. Different outcome of allogeneic transplantation in myelofibrosis using conventional or reduced-intensity conditioning regimens. Br J Haematol. 2006;135:367–373.
9. Wang JC, Chang TH, Goldberg A, Novetsky AD, Lichter S, Lipton J. Quantitative analysis of growth factor production in the mechanism of fibrosis in agnogenic myeloid metaplasia. Exp Hematol. 2006;34:1617–1623.
10. Chagraoui H, Komura E, Tulliez M, Giraudier S, Vainchenker W, Wendling F. Prominent role of TGF-beta 1 in thrombopoietin-induced myelofibrosis in mice. Blood. 2002;100:3495–3503.
11. Tefferi A, Vaidya R, Caramazza D, Finke C, Lasho T, Pardanani A. Circulating interleukin (IL)-8, IL-2R, IL-12, and IL-15 levels are independently prognostic in primary myelofibrosis: A comprehensive cytokine profiling study. J Clin Oncol. 2011;29:1356–1363.
12. Ciurea SO, Merchant D, Mahmud N, et al. Pivotal contributions of megakaryocytes to the biology of idiopathic myelofibrosis. Blood. 2007;110:986–993.
13. Harrison JS, Corcoran KE, Joshi D, Sophacleus C, Rameshwar P. Peripheral monocytes and CD4+ cells are potential sources for increased circulating levels of TGF-beta and substance P in autoimmune myelofibrosis. Am J Hematol. 2006;81:51–58.
14. Chang VT, Yook C, Rameshwar P. Synergism between fibronectin and transforming growth factor-beta1 in the production of substance P in monocytes of patients with myelofibrosis. Leuk Lymphoma. 2013;54:631–638.
15. Balduini A, Badalucco S, Pugliano MT, et al. In vitro megakaryocyte differentiation and proplatelet formation in Ph-negative classical myeloproliferative neoplasms: distinct patterns in the different clinical phenotypes. PLoS One. 2011;6:e21015.
16. Wang X, Prakash S, Lu M, et al. Spleens of myelofibrosis patients contain malignant hematopoietic stem cells. J Clin Invest. 2012;122:3888–3899.
17. Takayama N, Nishikii H, Usui J, et al. Generation of functional platelets from human embryonic stem cells in vitro via ES-sacs, VEGF-promoted structures that concentrate hematopoietic progenitors. Blood. 2008;111:5298–5306.
18. Takayama N, Nishimura S, Nakamura S, et al. Transient activation of c-MYC expression is critical for efficient platelet generation from human induced pluripotent stem cells. J Exp Med. 2010;207:2817–2830.
19. Ye Z, Zhan H, Mali P, et al. Human-induced pluripotent stem cells from blood cells of healthy donors and patients with acquired blood disorders. Blood. 2009;114:5473–5480.
20. Kumano K, Arai S, Hosoi M, et al. Generation of induced pluripotent stem cells from primary chronic myelogenous leukemia patient samples. Blood. 2012;119:6234–6242.
21. Mahalingam D, Kong CM, Lai J, Tay LL, Yang H, Wang X. Reversal of aberrant cancer methylome and transcriptome upon direct reprogramming of lung cancer cells. Sci Rep. 2012;2:592.
22. Okabe M, Otsu M, Ahn DH, et al. Definitive proof for direct reprogramming of hematopoietic cells to pluripotency. Blood. 2009;114:1764–1767.
23. Kuhlmann UC, Chwieralski CE, Reinhold D, Welte T, Buhling F. Radiation-induced matrix production of lung fibroblasts is regulated by interleukin-8. Int J Radiat Biol. 2009;85:138–143.
24. Le Bousse-Kerdiles MC, Martyre MC. Dual implication of fibrogenic cytokines in the pathogenesis of fibrosis and myeloproliferation in myeloid metaplasia with myelofibrosis. Ann Hematol. 1999;78:437–444.
25. Dong M, Blobe GC. Role of transforming growth factor-beta in hematologic malignancies. Blood. 2006;107:4589–4596.
26. Skov V, Larsen TS, Thomassen M, et al. Molecular profiling of peripheral blood cells from patients with polycythemia vera and related neoplasms: Identification of deregulated genes of significance for inflammation and immune surveillance. Leuk Res. 2012;36:1387–1392.

nature COMMUNICATIONS

ARTICLE

Received 29 Jan 2014 | Accepted 21 Jul 2014 | Published 27 Aug 2014

DOI: 10.1038/ncomms5770

Recurrent *CDC25C* mutations drive malignant transformation in FPD/AML

Akihide Yoshimi[1,*], Takashi Toya[1,*], Masahito Kawazu[2], Toshihide Ueno[3], Ayato Tsukamoto[1], Hiromitsu Iizuka[1], Masahiro Nakagawa[1], Yasuhito Nannya[1], Shunya Arai[1], Hironori Harada[4], Kensuke Usuki[5], Yasuhide Hayashi[6], Etsuro Ito[7], Keita Kirito[8], Hideaki Nakajima[9], Motoshi Ichikawa[1], Hiroyuki Mano[3] & Mineo Kurokawa[1]

Familial platelet disorder (FPD) with predisposition to acute myelogenous leukaemia (AML) is characterized by platelet defects with a propensity for the development of haematological malignancies. Its molecular pathogenesis is poorly understood, except for the role of germline *RUNX1* mutations. Here we show that *CDC25C* mutations are frequently found in FPD/AML patients (53%). Mutated CDC25C disrupts the G2/M checkpoint and promotes cell cycle progression even in the presence of DNA damage, suggesting a critical role for CDC25C in malignant transformation in FPD/AML. The predicted hierarchical architecture shows that *CDC25C* mutations define a founding pre-leukaemic clone, followed by stepwise acquisition of subclonal mutations that contribute to leukaemia progression. In three of seven individuals with *CDC25C* mutations, *GATA2* is the target of subsequent mutation. Thus, *CDC25C* is a novel gene target identified in haematological malignancies. *CDC25C* is also useful as a clinical biomarker that predicts progression of FPD/AML in the early stage.

[1] Department of Hematology and Oncology, Graduate School of Medicine, The University of Tokyo, 7-3-1 Hongo, Bunkyo-ku, Tokyo 113-8655, Japan. [2] Department of Medical Genomics, Graduate School of Medicine, The University of Tokyo, 7-3-1 Hongo, Bunkyo-ku, Tokyo 113-8655, Japan. [3] Department of Cellular Signaling, Graduate School of Medicine, The University of Tokyo, 7-3-1 Hongo, Bunkyo-ku, Tokyo 113-8655, Japan. [4] Department of Hematology, Juntendo University School of Medicine, 3-1-3 Hongo, Bunkyo-ku, Tokyo 113-8431, Japan. [5] Department of Hematology, NTT Medical Center Tokyo, 5-9-22 Higashi-Gotanda, Shinagawa-ku, Tokyo 141-8625, Japan. [6] Department of Hematology/Oncology, Gunma Children's Medical Center, 779 Simohakoda, Kitaakebonocho, Shibukawa-shi, Gunma 377-8577, Japan. [7] Department of Pediatrics, Graduate School of Medicine, Hirosaki University, 53 Honmachi, Hirosaki-shi, Aomori 036-8563, Japan. [8] Department of Hematology and Oncology, University of Yamanashi, 1110 Simokawakita, Chuou-shi, Yamanashi 409-3898, Japan. [9] Division of Hematology, Department of Internal Medicine, Keio University School of Medicine, 35 Shinanomachi, Shinjyuku-ku, Tokyo 160-8582, Japan. * These authors contributed equally to this work. Correspondence and requests for materials should be addressed to M.K. (email: kurokawa-tky@umin.ac.jp).

Familial platelet disorder (FPD)/acute myelogenous leukaemia (AML) (MIM601399) is an autosomal dominant disorder with inherited thrombocytopenia, abnormal platelet function and a lifelong risk of the development of a variety of haematological malignancies[1], such as AML, myelodysplastic syndromes (MDS) and myeloproliferative neoplasms. Although inherited *RUNX1* mutations are the cause of the congenital thrombocytopenia, it remains unclear whether a mutation in *RUNX1*, which is generally known to have a dominant-negative effect[2–4], is sufficient to induce the development of haematological malignancies in individuals with FPD/AML. It is also not known whether additional gene mutations are required for the transformation, and, if so, which genes are involved. Given that only 40% of FPD/AML patients develop these neoplasms[5] and that a relatively long period is required for subsequent *RUNX1* mutation-mediated development of neoplasms in FPD/AML, the secondary genetic events may function as a driver to promote malignant transformation. We reasoned that identifying gene mutations responsible for the malignant transformation of FPD/AML would provide indispensable information for addressing these questions. However, only about 30 pedigrees with FPD/AML have been reported so far, and the rarity of this disorder has impeded the establishment of clinical diagnostic criteria and the clinical improvement to refine cancer therapy and to identify biomarkers that would allow detection of patients at risk for the onset of malignancies in FPD/AML.

We collected DNA samples and clinical information of 73 individuals, belonging to 57 pedigrees, who have a history of familial thrombocytopenia and/or haematological malignancies, with the aim of identifying pedigrees with FPD/AML and uncovering recurrent mutations that drive the malignant transformation. Next-generation sequencing and single-cell sequencing strategy suggest that somatic mutation in *CDC25C* may be one of the early genetic events for leukaemic initiation in FPD/AML, and further stepwise acquisition of mutations such as *GATA2* leads to FPD/AML-associated leukaemic progression. These observations shed light on a part of leukemogenesis in FPD/AML.

Results

A novel gene target in haematological disorders. Thirteen patients in 7 pedigrees were diagnosed as having FPD/AML after screening for germline *RUNX1* mutations in 73 index patients; 7 of the 13 patients had developed haematological malignancies, while the other 6 only showed thrombocytopenia (Table 1). Most of the detected *RUNX1* mutations were point mutation in Runt homology domain or frame-shift mutation that lost transactivation domain, consistent with the previous reports[2,4]. As haploinsufficiency of *RUNX1* might cause familial thrombocytopenia with propensity to develop AML[1], we also examined whether the pedigrees have *RUNX1* loss of heterozygosity (LOH) or not. A synchronized quantitative-PCR method[6] and single-nucleotide polymorphism (SNP) sequencing detected no case with LOH in *RUNX1* in our cohort (Supplementary Fig. 1 and detailed in Methods). To systematically identify additional genetic alterations, we utilized whole-exome sequencing for two individuals from the same FPD/AML pedigree who shared a common *RUNX1*_p.Phe303fs mutation and who had developed MDS (subject 20) or myelofibrosis (subject 21) at the age of 37 and 17 years, respectively. In both these patients, the disease had progressed to AML[7]. Validation by Sanger sequencing and/or targeted deep sequencing of candidate mutations in paired tumour/normal DNA samples confirmed 10 (subject 20) and 8 (subject 21) somatically acquired nonsynonymous mutations (Table 2; Supplementary Figs 2–4; Supplementary Methods). Surprisingly, both patients carried the identical somatic *CDC25C* mutation (p.Asp234Gly), which had not been reported previously in human cancers (Fig. 1a,b). Prompted by this finding, we investigated *CDC25C* mutations in other FPD/AML cases by deep sequencing. In total, four of seven affected patients with haematological malignancies had *CDC25C* mutations, of which three carried the same p.Asp234Gly mutation. Moreover, *CDC25C* mutations were detected in an additional three FPD/AML patients who had not yet developed haematological malignancies, although the variant allele fractions (VAFs) were much lower in this group of patients than in those who had already developed haematological malignancies (Fig. 1c; Table 1). Thus, 7 of the 13 FPD/AML patients (53%) harboured a *CDC25C* mutation. *CDC25C* was also screened for mutations in 90 sporadic MDS and 53 AML patients, including 13 MDS and 3 AML cases who carried *RUNX1* mutations. No *CDC25C* mutations were identified in the 90 sporadic cases, except for the p.Ala344Val in an MDS patient bearing a *RUNX1* mutation, indicating that *CDC25C* mutations were significantly associated with germline, but not with somatic *RUNX1* mutations ($P = 0.004$; Supplementary Fig. 5; Supplementary Table 1).

Clonal evolution of FPD/AML. Deep sequencing of individual mutations that had been detected by whole-exome sequencing

Table 1 | Mutational status of *CDC25C* in FPD/AML patients.

Pedigree number	Subject number	RUNX1 mutation	Disease status	Age, years*	CDC25C mutation	VAF (%)
18	20	p.Phe303fs	MDS/AML	37/38	p.Asp234Gly	31.7/45.8
	21		MF/AML	17/18	p.Asp234Gly	31.1/39.0
19	22	p.Arg174*	AML	41	p.His437Asn	39.7
54	65	p.Ser140Asn	MDS	25	—	—
	66		AML	56	p.Asp234Gly	24.2
32	38	p.Leu445Pro	HCL	72	—	—
16	18	p.Thr233fs	Thrombocytopenia	—	p.Asp234Gly	5.9
53	62	p.Gly262fs	MDS	12	—	—
	63		Thrombocytopenia	—	—	—
	67		Thrombocytopenia	—	—	—
57	71	p.Gly172Glu	Pancytopenia†	—	p.Asp234Gly	8.3
	72		Thrombocytopenia	—	—	—
	73		Thrombocytopenia	—	p.Lys233Glu	1.8

AML, acute myeloid leukemia; FPD, familial platelet disorder; HCL, hairy cell leukemia; MDS, myelodysplastic syndrome; MF, myelofibrosis; VAF, variant allele fraction.
*Age at the time of diagnosis of each haematological malignancy is shown.
†Thrombocytopenia, leukopenia and iron-deficiency anemia were diagnosed.

Table 2 | Validated somatic mutations.

Gene symbol	Ref seq_no.	Amino-acid change	Position (hg19)	Base change	Mutation type	SIFT prediction	VAF at MDS/MF (%)	VAF at AML (%)
Subject 20								
AGAP4	NM_133446	p.Arg484Cys	g.chr10:46321905	C->T	Missense	Damaging	13.2	11.5
CDC25C	NM_001790	p.Asp234Gly	g.chr5:137627720	A->G	Missense	Damaging	31.7	45.8
CHEK2	NM_007194	p.Arg406His	g.chr22:29091740	G->A	Missense	Tolerated	14.6	11.1
COL9A1	NM_001851	p.Gly878Val	g.chr6:70926733	G->T	Missense	Damaging	9.6	26.4
DTX2	NM_001102594	p.Pro74Arg	g.chr7:76110047	C->G	Missense	Damaging	18.3	11.2
FAM22G	NM_001170741	p.Ser508Thr	g.chr9:99700727	T->A	Missense	Tolerated	10.2	27.6
GATA2	NM_001145661	p.Leu321His	g.chr3:128202758	T->A	Missense	Damaging	0.0	28.1
LPP	NM_001167671	p.Val538Met	g.chr3:188590453	G->A	Missense	Damaging	9.7	28.8
RP1L1	NM_178857	p.Ser215fs	g.chr8:10480295	insC	Frameshift	Damaging	14.2	12.7
SIGLEC9	NM_014441	p.Ser437Gly	g.chr19:51633253	A->G	Missense	Tolerated	27.4	42.5
Subject 21								
ANXA8L1	NM_001098845	p.Val281Ala	g.chr10:48268018	T->C	Missense	Damaging	30.8	36.8
CDC25C	NM_001790	p.Asp234Gly	g.chr5:137627720	A->G	Missense	Damaging	31.1	39.1
DENND5A	NM_001243254	p.Arg320Ser	g.chr11:9215218	A->C	Missense	Damaging	29.5	37.3
FER	NM_005246	p.Tyr634Cys	g.chr5:108382876	A->G	Missense	Damaging	1.4	30.4
FNDC1	NM_032532	p.Arg189Cys	g.chr6:159636081	C->T	Missense	Damaging	29.3	35.9
OR8U1	NM_001005204	p.Asn175Ile	g.chr11:56143623	A->T	Missense	Damaging	30.0	34.1
PIDD	NM_145886	p.Arg342Cys	g.chr11:802347	C->T	Missense	Damaging	3.3	28.3
ZNF614	NM_025040	p.Glu202Gly	g.chr19:52520246	A->G	Missense	Damaging	28.7	33.7

AML, acute myeloid leukemia; MDS, myelodysplastic syndrome; MF, myelofibrosis; SIFT, sorting intolerant from tolerant; VAF, variant allele fraction.

allowed accurate determination of their VAFs; on this basis, we could establish an inferred model of clonal evolution in terms of individual mutations in subjects 20 and 21 (Fig. 2a,b; Supplementary Fig. 6a,b). Intratumoral heterogeneity was evident at both MDS and AML phases in subject 20. According to the predicted model, a founding clone with a *CDC25C* mutation acquired additional mutations in *COL9A1*, *FAM22G* and *LPP* (group A), followed by the emergence of a *GATA2* mutation (group B), which was associated with leukaemic transformation, whereas the size of another subclone, defined by mutations in *CHEK2* and three other genes (group C), was unchanged. To validate this hierarchical model, single-cell genomic sequencing was performed using genomic DNA of 63 bone marrow cells from subject 20 when the patient was in the AML phase. Assuming that all cells harbour the *RUNX1* mutation, the false-negative rate of the procedure reached 35%, possibly due to biased allele amplification (Online Methods). However, this technique successfully demonstrated that the group A/B and group C mutations were mutually exclusive (Fig. 2c; Supplementary Table 2). To statistically evaluate this possibility, we assumed two hypotheses (H_0: the mutational status of genes in group A/B and group C is independent; H_1: mutations in group A/B and group C are mutually exclusive) and calculated each probability distribution (P_i: probability that the current results as shown in Fig. 2c were obtained under the hypothesis H_i). Our mutational profile data were achieved with a much higher likelihood under H_1 than H_0 (Supplementary Fig. 7 and detailed in Supplementary Methods). Similarly, the clonal architecture for subject 21 was portrayed in Fig. 2b and Supplementary Fig. 6b. In both scenarios, *CDC25C* mutations seemed to represent a founding mutation with the highest VAF, suggesting that the *CDC25C* mutation contributed to the establishment of a founding tumour population as an early genetic event, whereas progression to AML seemed to be accompanied by the appearance of additional mutations, indicating a multistep process in leukemogenesis.

Along with the somatic mutations found in subjects 20 and 21, a *GATA2* mutation was also identified in subject 22 (Fig. 3a). This patient developed AML with multilineage dysplasia, which led to the diagnosis of AML – MRC (myelodysplasia-related changes). Remission-induction therapies were only partially effective and the blast cell count was reduced from 54 to 5.6%, while dysplastic features persisted (Fig. 3b; Supplementary Fig. 8). Allogeneic stem cell transplantation was successfully performed from a human leukocyte antigen-matched unrelated donor and durable complete remission, with 100% donor chimerism, was achieved. During treatment, the VAF of the *GATA2* mutation decreased virtually in parallel with the blast cell percentage, while the VAF of the *CDC25C* mutation hovered at a high level before transplantation. Thus, we hypothesized that the *GATA2* mutation induced leukaemia progression in this patient, whereas the *CDC25C* mutation was associated with the pre-leukaemic status. Another *GATA2* mutation (p.Leu359Val) was found in subject 18, with a VAF (0.94%), who showed only thrombocytopenia without any signs of leukaemia progression and who had a small subclone with a concurrent *CDC25C* mutation (Fig. 3c). Although *GATA2* mutations are detected in a small number of patients with FPD/AML, the findings described above suggest that mutation of *GATA2* is a key factor promoting disease progression in FPD/AML (Fig. 3d).

Biological consequences of *CDC25C* mutations. We next investigated the possible impact of *CDC25C* mutation on clonal selection and evolution. CDC25C is a phosphatase that prevents premature mitosis in response to DNA damage at the G2/M checkpoint, while it is constitutively phosphorylated at Ser216 throughout interphase by c-TAK1 (refs 8–10). When phosphorylated at Ser216, CDC25C binds to 14-3-3 protein[11], leading to sequestration of CDC25C to the cytoplasm and its inactivation. Ba/F3 cells were transduced with retroviruses encoding the wild-type or mutant CDC25C containing each of the individual mutations (p.Asp234Gly, p.Ala344Val, p.His437Asn and p.Ser216Ala), and assayed for the phosphorylation status, 14-3-3 protein-binding capacity and intracellular localization of each of these proteins. The Ser216Ala mutant form

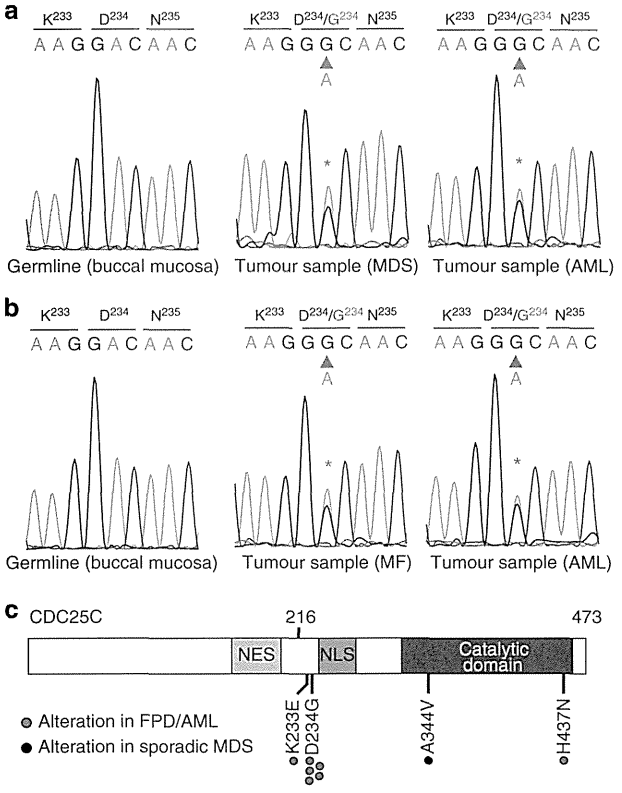

Figure 1 | Mutation in *CDC25C* recurs in cases of FPD/AML. (**a**,**b**) Sanger sequencing of *CDC25C* mutations found in whole-exome sequencing is shown. Both forward and reverse traces were available for each mutation, but only one trace is shown above. The results of buccal mucosa, pre-leukaemic phase and leukaemic phase is demonstrated for subject 20 (**a**) and subject 21 (**b**), respectively. (**c**) The distribution of alterations is shown for the CDC25C protein. NES, a putative nuclear export signal domain between amino acids 177–200; NLS, a putative nuclear localization sequence domain consisting of amino acids 240–244.

of CDC25C, which lacks the phosphorylation site, was used as a negative control. In all of the mutated forms of CDC25C, the capacity for binding to c-TAK1 was reduced (Fig. 4a,b; Supplementary Fig. 9a,b), resulting in decreased phosphorylation of CDC25C at Ser216 (Fig. 4c). Consequently, the mutant proteins failed to bind 14-3-3 protein efficiently (Fig. 4d,e; Supplementary Fig. 8c,d) and remained in the nucleus even during interphase (Fig. 4f; Supplementary Figs 10 and 11). In accordance with these observations, CDC25C mutants enhanced mitotic entry, which was exaggerated by low-dose radiation-induced DNA damage (Fig. 4g,h; Supplementary Fig. 12; Supplementary Methods). These results suggest that mutation of *CDC25C* results in disruption of the DNA checkpoint machinery. Next, we investigated why mutation of *CDC25C* is a frequent genetic event in FPD/AML. It is known that *RUNX1* mutations suppress DNA damage repair and subsequent cell cycle arrest in hematopoietic cells by means of transcriptional suppression of several genes that are involved in DNA repair[12,13]. We confirmed that FPD/AML-associated *RUNX1* mutations have similar effects, as we observed activation of the G2/M checkpoint mechanism in the presence of *RUNX1* mutations (Fig. 4i; Supplementary Fig. 13a,b). We found, however, that introduction of mutations in *CDC25C* resulted in enhanced mitosis entry, despite co-existence of *RUNX1* mutations (Fig. 4i). Therefore, we speculated that compromised DNA damage checkpoint mechanisms caused by mutations in *CDC25C* may contribute to malignant transformation, in concert with increased genomic instability due to *RUNX1* mutations.

Discussion

Whole-exome sequencing, followed by targeted deep sequencing, identified novel aspects of the pathogenesis of malignant transformation in FPD/AML. First, the high frequency of *CDC25C* mutations in FPD/AML underscores their major role in the development of haematological malignancies in FPD/AML patients. To our knowledge, *CDC25C* mutations have not been reported previously and represent a new recurrent mutational target in haematological malignancies, although *CDC25C* mutations have been reported in some solid carcinomas with unknown significance[14,15]. Furthermore, our functional assays support their biological significance, which is characterized by cell cycle progression and premature mitotic entry. Although the 5q31 minimally deleted region, in which CDC25C is located, is frequently detected in MDS, it seems to be associated with other oncogenic mechanisms since our functional assays suggested that *CDC25C* mutations in FPD/AML were gain-of-function type mutations that facilitate the mitotic entry by aberrant accumulation in the nucleus. Impaired DNA repair function mediated by germline *RUNX1* mutation may play a role in the generation of *CDC25C* mutations.

Evaluation of the allelic burden of mutated genes demonstrated that *CDC25* mutations are found with high VAFs in FPD/AML-derived leukaemia and with low VAFs in cases of thrombocytopenia. Our hierarchical model and clonal selection highlighted that mutation of *CDC25C* defines an initial event during malignant transformation and predates subclonal mutations in *GATA2* and other genes. On the basis of the observation that four of the seven FPD/AML patients with *CDC25C* mutations have developed leukaemia and that *CDC25C* mutations were actually detected in the leukaemic subclones, we speculated that a FPD/AML patient with a *CDC25C* mutation, but without clinically evident leukaemia, is at high risk for the onset of leukaemic progression. Examination of the allelic burden of *CDC25C* mutation may thus serve to evaluate the risk of leukaemic progression in patients with FPD/AML.

Among the mutations found in FPD/AML, mutations in *GATA2* were identified in 3 of 13 individuals (subjects 18, 20 and 22). *GATA2* mutations were frequently identified in FPD/AML-derived leukaemia (2/7) and in a patient with thrombocytopenia who had a small subclone bearing a *CDC25C* mutation (1/6). Although reports on the clinical relevance of *GATA2* mutations in myeloid malignancy are limited, several lines of evidence in this respect have recently been reported. *GATA2* mutations are frequently found in a subgroup of patients with cytogenetically normal AML with biallelic *CEBPA* gene mutations[16], which account for ~4% of AML. Germline *GATA2* mutations are also observed in disorders linked to an increased propensity for the development of MDS and AML, including Emberger syndrome, MonoMAC syndrome and dendritic cells, monocytes, B and natural killer cells deficiency[17–20]. The alterations in *GATA2* (leading to p.Leu321His and p.Leu359Val), which were found in FPD/AML patients in this study, are located in the part of the gene encoding the N-terminal and C-terminal zinc-finger domains, respectively (Fig. 3d). Mutations affecting the identical amino acids have been reported in AML patients bearing *CEBPA* mutations and chronic myeloid leukaemia patients in blast crisis[16,21]. Thus, *GATA2* mutation may contribute to AML progression in collaboration with *RUNX1* and/or *CDC25C* mutations. Furthermore, although

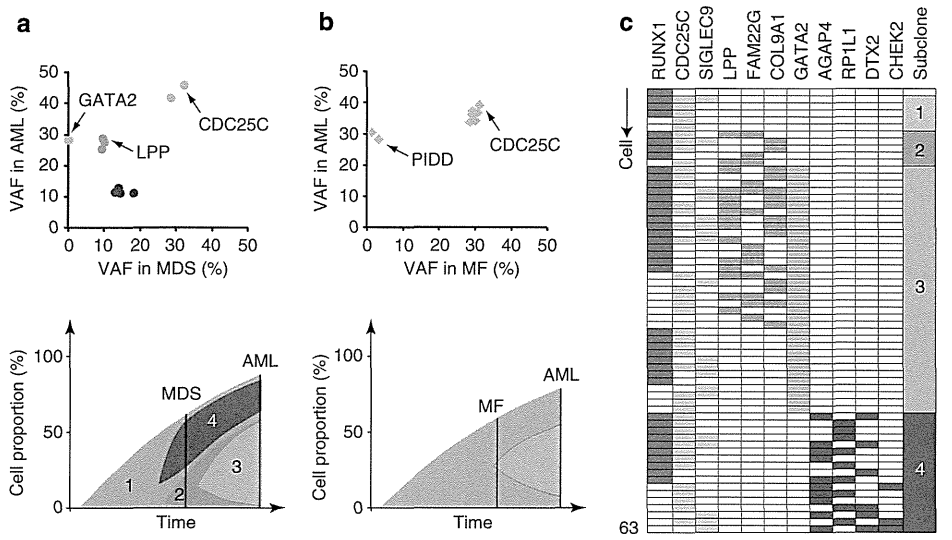

Figure 2 | Clonal evolution of FPD/AML-related myeloid disorders. (**a**,**b**) Observed variant allele fraction (VAF) of validated mutations are listed in Table 2, in both pre-leukaemic and leukaemic phases, are shown in diagonal plots (top) for subject 20 (**a**) and subject 21 (**b**). Predicted chronological behaviours in different leukemia subclones are depicted below each diagonal plot. Distinct mutation clusters are displayed by colour. The vertical axis represents cell proportion of each clone calculated by VAF × 2 (%) (because all the mutations were heterozygous), regarding the whole bone marrow as 100%. (**c**) Mutation status of each bone marrow cell from subject 20 during the acute myeloid leukemia (AML) phase. The vertical axis represents each cell ($n = 63$) and the horizontal axis displays each gene mutation. Coloured columns show that the corresponding cell harbours gene mutation(s) as defined in Online Methods. Subclone numbers shown in the right row correspond to the numbers in the lower figure of **a**.

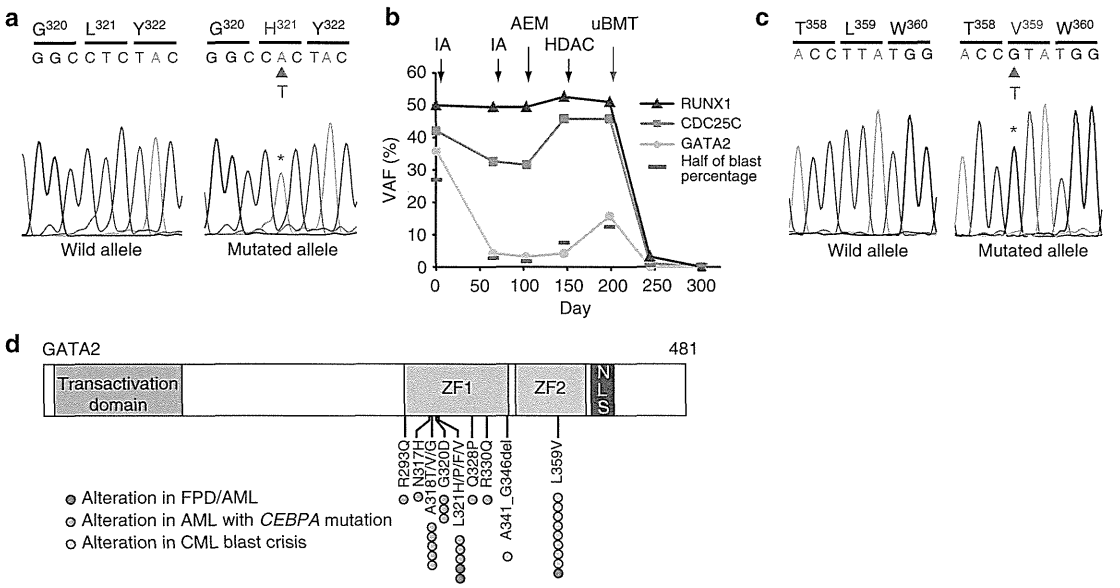

Figure 3 | *GATA2* mutations in FPD/AML. The result of Sanger sequencing for *GATA2* p.Leu321His mutation in subject 22 (**a**) and Leu359Val mutation in subject 18 (**c**) validated with subcloning strategy by methods shown in Supplementary Methods. (**b**) Variant allele fractions (VAFs) of *RUNX1*, *CDC25C* and *GATA2* mutation in subject 22 are demonstrated with the time course of treatment. Half the value of the blast cell percentage, which corresponds to the allele frequency of a heterozygous mutation, is also shown by a red bar. IA, idarubicine + Ara-C; AEM, Ara-C + etoposide + mitoxantrone; HDAC, high-dose Ara-C; uBMT, unrelated bone marrow transplantation. (**d**) Schematic representation of *GATA2* mutations. *GATA2* mutations that were identified in FPD/AML are displayed together with mutations found in AML with *CEBPA* mutation[16] as well as in CML patients in blast crisis[21]. ZF, zinc-finger domain; NLS, a putative nuclear localization sequence domain.

another report identified somatic *CBL* mutation with acquired 11q uniparental disomy as a second hit as being responsible for leukaemic transformation in FPD/AML[22], *CBL* mutations were not detected in our series of FPD/AML samples.

Although the precise pathogenetic roles of *CDC25C* mutations remain unclear, we presume that mutant CDC25C alleles confer a proliferative advantage under certain circumstances in which DNA repair machinery is compromised, such as that mediated by

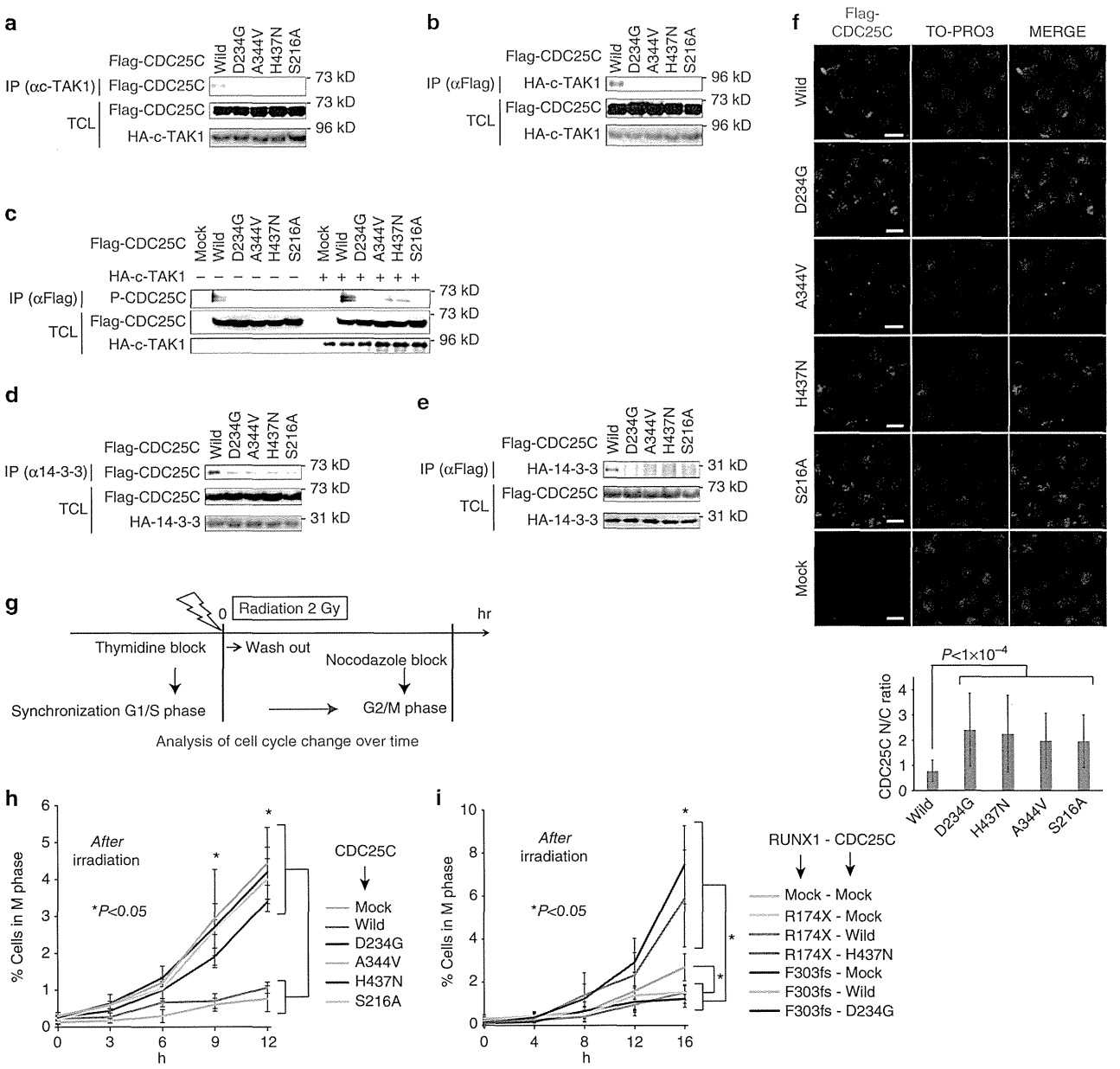

Figure 4 | Mutated CDC25C enhances mitotic entry. (**a**) HEK293T cells were transiently transfected with constructs encoding Flag-tagged CDC25C wild type or mutants, as indicated, and cell lysates were immunoprecipitated with anti-c-TAK1 antibody. Binding capacity of CDC25C was evaluated by western blotting. IP, immunoprecipitation; TCL, total cell lysate. (**b**) Reciprocal immunoprecipitation of **a** using anti-Flag (CDC25C) antibody for immunoprecipitation. (**c**) Left half; cell lysates were immunoprecipitated with anti-Flag antibody. Phosphorylation levels of CDC25C were assessed by phosphorylated-Ser216-specific anti-CDC25C antibody. Right half; the same experiment was performed with cell lysates from HEK293T cells transfected with constructs encoding Flag-tagged CDC25C wild type or mutants and HA-tagged c-TAK1. (**d**) Mutated CDC25C showed reduced capacity for binding to 14-3-3. Cell lysates were immunoprecipitated with anti-14-3-3 antibody and binding capacity of CDC25C was evaluated. (**e**) Reciprocal immunoprecipitation of **d** using anti-Flag (CDC25C) antibody for immunoprecipitation. (**f**) Localization of CDC25C or its mutants was visualized by immunofluorescence. Anti-Flag antibody and Alexa Fluor 555 antibody was used for visualization of CDC25C. N/C ratio of each cell was calculated as detailed in Supplementary Methods and Supplementary Fig. 10. The mean and s.d. of the N/C ratio is presented. Statistical significance of difference was determined by unpaired Student's *t*-test ($n>30$ for each). Scale bar, 10 μm. (**g**) Schematic description of the method used for evaluation of mitotic entry. (**h**) Mitotic entry of CDC25C-mutated cells. Percentage of mutated CDC25C-transduced cells in the M phase was compared with that of wild-type CDC25C-transduced cells. *P* values were calculated using Student's *t*-test and the differences between groups, as indicated, were all statistically significant ($^*P<0.05$) at 10 and 12 h after irradiation ($n=3$). The average and s.d. is presented. (**i**) Mutated RUNX1 and CDC25C were co-expressed in Ba/F3 cells, as indicated, and mitosis entry of these cells was evaluated. The differences between groups, as indicated, were all statistically significant ($^*P<0.05$ at 16 h after washout of thymidine ($n=3$). *P* values were determined using the Student's *t*-test. The average and s.d. is presented.

a germline *RUNX1* mutation. In addition, as Turowski and colleagues reported that CDC25C was involved in S phase entry in addition to mitotic entry[23], release from thymidine-induced G1/S block may be affected by some unknown machinery mediated by mutated CDC25Cs, which might affect the results when we observed G2/M phase fraction of these cells. It is not clear why *CDC25C* mutations are repetitively documented in FPD/AML, but not in sporadic MDS or AML cases. One possibility is that in the presence of a *RUNX1* mutation, as an initial event, an extended period is required before an additional *CDC25C* mutation is acquired. This proposal is supported by the clinical observation that ~40% of patients with FPD/AML develop leukaemia in their 30s[5]; however, the mutational status in *CDC25C* in the reported cohort was unknown.

One of the important problems in the research of FPD/AML is that definitive diagnostic criteria have not been established yet. For this purpose, more extensive studies are required for accumulating clinical characterization, genetic information and functional examination as to whether a *RUNX1* variant in families with thrombocytopenia and/or haematological malignancy is causal[24]. We clarified tentative diagnostic criteria for FPD/AML, which was used in this study (in Methods). Regarding the three missense variants in our study (p.Ser140Asn in pedigree 54, p.Gly172Glu in pedigree 57 and p.Leu445Pro in pedigree 32), Ser140 and Gly172 have been reported to be mutated in sporadic AML and/or MDS cases[25,26]. In addition, induced pluripotent stem cells from a FPD/AML pedigree with p.Gly172Glu recapitulate the phenotype of FPD/AML after hematopoietic differentiation[27]. Ser140 has been also shown to be important for RUNX1 conformation, and a mutation of this site affects hydrogen bonds and results in functional loss[28,29]. Furthermore, all the three missense variants have not been reported in the following SNP database: SNP database (dbSNP) (http://www.ncbi.nlm.nih.gov/projects/SNP), the 1000 Genomes Project (http://www.1000genomes.org), HGVB (http://www.genome.med.kyoto-u.ac.jp/SnpDB/index.html). They were also predicted as 'damaging' by Polyphen-2 (http://genetics.bwh.harvard.edu/pph2/), SIFT (http://sift.jcvi.org/) and PROVEAN (http://provean.jcvi.org/index.php). Therefore, we regarded the pedigrees with these *RUNX1* variants as having FPD/AML in this study. However, regarding pedigree 32 with p.Leu445Pro, we could not completely exclude the possibility of incidental co-occurrence of a possible non-causal *RUNX1* germline variant and hairy cell leukaemia, although co-occurrence of them is supposed to be rare. In addition, we should bear in mind the somatic as well as germline LOH of *RUNX1*, which contributes to thrombocytopenia and/or leukemogenesis in FPD/AML.

In conclusion, our results indicate that FPD/AML-associated leukaemic transformation is due to stepwise acquisition of mutations and clonal selection, which is initiated by a *CDC25C* mutation in the pre-leukaemic phase, and is further driven by mutations in other genes including *GATA2* (Supplementary Fig. 14). The identification of *CDC25C* as the target gene responsible for the leukaemic transformation will facilitate diagnosis and monitoring of individuals with FPD/AML, who are at an increased risk of developing life-threatening haematological malignancy.

Methods

Subjects. Studies involving human subjects were done in accordance with the ethical guidelines for biomedical research involving human subjects, which was developed by the Ministry of Health, Labour and Welfare, Japan; the Ministry of Education, Culture, Sports, Science, and Technology, Japan; and the Ministry of Economy, Trade, and Industry, Japan, and enforced on 29 March 2001. This study was approved by ethical committee of the University of Tokyo and each participating institution. Written informed consent was obtained from all patients whose samples were collected after the guideline was enforced. All animal experiments were approved by the University of Tokyo Ethics Committee for Animal Experiments. The clinical data, peripheral blood sample and buccal mucosa of the patients whose pedigree contained two or more individuals with thrombocytopenia and/or any haematological malignancies were collected from participating institutions. Platelet threshold depended on each institution's judge and any haematological malignancies were allowed. The diagnoses were self-reported. When all the following four criteria were fulfilled, the patient was considered as having FPD/AML in this study: (1) the pedigree has two or more individuals with thrombocytopenia and/or any haematological malignancies; (2) a germline *RUNX1* variant, including missense, nonsense, frameshift, insertion and deletion, is confirmed by Sanger sequencing and a synchronized quantitative-PCR method in at least one family member; (3) the *RUNX1* variant has not been reported in public dbSNP; (4) no germline mutations were detected in the following 16 genes: *GATA2*, *GATA1*, *CEBPA*, *MPL*, *MYH9*, *MYL9*, *GP1BA*, *GP9*, *MASTL*, *HOXA11*, *CBL*, *DIDO1*, *TERT*, *ANKRD26*, *GFI1B* and *SRP72*. Regarding the last criterion, 16 genes were selected because they have been reported to be responsible for familial thrombocytopenia and/or haematological malignancies.

Whole-exome sequencing. Genomic DNA was extracted from samples using the QIAamp DNA Mini kit (Qiagen). Exome capture was performed. Enriched exome fragments were subjected to sequencing using HiSeq2000 (Illumina). We removed any potential somatic mutations that were observed in dbSNP (http://www.ncbi.nlm.nih.gov/projects/SNP) or in the 1000 Genomes Project (http://www.1000genomes.org) data. All candidate single-nucleotide variations and indels, which were predicted to be deleterious by the Polyphen-2 algorithm, were validated by deep sequencing and Sanger sequencing. Genomic DNA samples from the buccal mucosa of the two patients (subject 20 and subject 21) were used as references. All candidate somatic mutations were validated by Sanger sequence and deep sequencing using primers listed in Supplementary Tables 3 and 4.

Deep sequencing. Using genomic DNA of the patients as template, each targeted region was PCR amplified with specific primers (Supplementary Table 4). The amplification products from an individual sample were combined and purified with the AMpure XP Kit (Beckman Coulter) and library preparation was carried out using the Ion Xpress Fragment Library Kit (Life Technologies) according to the manufacturer's instructions. The Agilent 2100 Bioanalyzer (Agilent Technologies) and the associated High Sensitivity DNA kit (Agilent Technologies) were used to determine quality and concentration of the libraries. The amount of the library required for template preparation was calculated using the template dilution factor calculation described in the protocol. Emulsion PCR and enrichment steps were carried out using the Ion OneTouch 200 Template Kit v2 DL (Life Technologies). Sequencing was undertaken using Ion Torrent PGM and Ion 318 chips Kit v2 (Life Technologies). The Ion PGM 200 Sequencing Kit (Life Technologies) was used for sequencing reactions, following the recommended protocol. The presence of *CDC25C* and *GATA2* mutations was also validated by a subclone strategy for DNA sequence analysis.

Single-cell sequencing and genome amplification. Single cells were separated from the bone marrow of subject 20 at AML phase using FACSAria II (BD biosciences) (Supplementary Fig. 15a). Each cell was deposited into individual wells of a 96-well plate. Single cells were lysed and whole genome from single cell was amplified using GenomePlex Single Cell Whole-Genome Amplification Kit (Sigma-Aldrich). Mutation status of each gene was analysed by direct sequencing with specific primers (Supplementary Table 5). To improve the sensitivity of this procedure, we used multiple primer sets for detecting a single-nucleotide variation. We estimated the false-negative rate of this procedure based on the ratio of RUNX1 mutation, which is supposed to be observed in all of the cells. The false-negative rate was estimated to be 35% (22 cells out of 63 cells, Supplementary Table 2), which is consistent with the manufacturer's bulletin reporting the allelic dropout of 30%. In light of these results, we regard those cells with at least one gene mutation in a mutational group (coloured in red, orange, green, blue or purple) as being positive for gene mutations of the corresponding group. To assess whether mutations in *LPP*, *FAM22G*, *COL9A1* and *GATA2* and mutations in *AGAP4*, *RP1L1*, *DTX2* and *CHEK2* were mutually exclusive, we performed a statistical analysis as follows. First of all, we determine a matrix **A** that virtually represents the mutational status of eight genes (1: *LPP*, 2: *FAM22G*, 3: *COL9A1*, 4: *GATA2*, 5: *AGAP4*, 6: *RP1L1*, 7: *DTX2* and 8: *CHEK2*) of 57 cells. Concretely, **A** is defined as follows:

$$\mathbf{A}=\begin{pmatrix} a_{1,1} & \cdots & a_{8,1} \\ \vdots & \ddots & \vdots \\ a_{1,57} & \cdots & a_{8,57} \end{pmatrix} \quad a_{i,j}=\begin{cases} 0: \text{if gene i of cell j is wildtype} \\ 1: \text{if gene i of cell j is mutated} \end{cases} \qquad (1)$$

On the other hand, a matrix **R** indicates data from the actual experimental results of mutational analysis as shown in Fig. 2c. Elements of **R** is provided in

Supplementary Table 2.

$$\mathbf{R}=\begin{pmatrix} r_{1,1} & \cdots & r_{8,1} \\ \vdots & \ddots & \vdots \\ r_{1,57} & \cdots & r_{8,57} \end{pmatrix} \quad r_{i,j}=\begin{cases} 0: \text{if gene i of cell j is wild type} \\ 1: \text{if gene i of cell j is mutated} \\ 2: \text{if mutational status of gene i of cell j is undetermined} \end{cases} \tag{2}$$

Then we assumed two hypotheses: H_0 and H_1.

H_0: the mutational status of genes $1\sim4$ and genes $5\sim8$ is independent. Each matrix elements of **A** are randomly assigned 0 or 1 (at ratio of 1:1) independently of each other.

H_1: mutations in genes $1\sim4$ and genes $5\sim8$ are mutually exclusive, and cells $1\sim40$ harbour mutations of genes $1\sim4$, while cells $41\sim57$ harbour mutations of genes $5\sim8$. In mathematical representation,

$$a_{i,j}=\begin{cases} 0: (5\le i\le 8 \text{ and } 1\le j\le 40) \text{ and } (1\le i\le 4 \text{ and } 41\le j\le 57) \\ 0 \text{ or } 1 \text{ randomely}: (1\le i\le 4 \text{ and } 1\le j\le 40) \text{ and } (5\le i\le 8 \text{ and } 41\le j\le 57) \end{cases} \tag{3}$$

We assumed matrices $\mathbf{A}_0$ and $\mathbf{A}_1$ that represent virtually generated mutational status under the hypotheses H_0 and H_1, and calculate the probability of substantializing **R** for given $\mathbf{A}_0$ and $\mathbf{A}_1$.

$P_0(\mathbf{R}/\mathbf{A}_0)$ and $P_1(\mathbf{R}/\mathbf{A}_1)$ can be calculated for given matrices $\mathbf{A}_0$ and $\mathbf{A}_1$ under the condition as follows:

Probability that we cannot determine whether a cell has mutation in gene X when the cell does not actually have a mutation; 28% (based on our data shown in Supplementary Table 2).

Probability that we judge that a cell has a mutation in gene X when the cell does not actually have a mutation; 5% (because it is very unlikely to happen).

Probability that we can judge correctly that a cell does not have a mutation in gene X when the cell does not actually have a mutation; 67% ($100-28-5=67\%$).

Probability that we cannot determine whether a cell has mutation in gene X when the cell actually has a mutation; 28% (based on our data shown in Supplementary Table 2).

Probability that we judge that a cell has a mutation in gene X when the cell actually has a mutation; 35% (the estimated false-negative rate based on the ratio of *RUNX1* mutation).

Probability that we can judge correctly that a cell has a mutation in gene X when the cell actually has a mutation; 37% ($100-28-35=37\%$).

Put it simply, $\mathbf{P}_0$ represents the probability that one can get the mutational profile R when a cell harbours mutations independently of each other, while $\mathbf{P}_1$ indicates the probability that R is realized under the condition where mutations in gene groups $1\sim4$ and $5\sim8$ are exclusive. Because $\mathbf{A}_0$ and $\mathbf{A}_1$ that meet the hypotheses H_0 and H_1 can be generated innumerably, we conducted a computational simulation to acquire the distribution of P_0 and P_1 by generating $\mathbf{A}_0$ and $\mathbf{A}_1$ 100,000 times. For visibility, horizontal axis is converted to $-\ln(P)$.

Synchronized quantitative-PCR. These experiments were performed mostly as described previously[6]. Briefly, genomic DNA was denatured 95 °C for 5 min and iced immediately. Using the LightCycler 480 Instrument II (Roche), thermal cycling was performed with denatured genomic DNA, forward and reverse primers (Supplementary Table 6), THUNDERBIRD SYBR qPCR mix (TOYOBO). Threshold cycle scores were determined as the average of triplicate samples. We designed 27 primers for *RUNX1* and 3 reproducible primers (that is, primer RUNX-9, RUNX-19 and RUNX-20) were chosen by preparatory experiments. RPL5-2 and PRS7-1 primers, which were authorized previously[6], were also utilized as controls. In addition, genomic DNA extracted from the bone marrow sample of a MDS patient with a chromosome 21 deletion was also examined with the same primers as a control of *RUNX1* locus copy-number loss. Crossing points (Cps) of designed primers were examined by quantitative PCR. *RUNX1* locus copy-number relative to RPL5-2 was calculated using Cps of RUNX-9 and RPL5-2, with RPL5-2 values set at 2. Similar results were obtained when Cps of RUNX-19, RUNX-20 or RPS7-1 values were used.

LOH detection with SNP sequencing. To examine the existence of uniparental disomy, we designed four specific primers to detect nine SNPs in *RUNX1*, which are frequently seen (>40%) (Supplementary Table 7). Direct sequencing was performed with the primers, and heterogeneity of SNPs was examined.

Chemicals and immunological reagents. Thymidine and nocodazole were purchased from Sigma-Aldrich. Anti-CDC25C, anti-phospho-CDC25C (Ser216) and anti-beta-actin antibodies were purchased from Cell Signaling Technology. Anti-HA monoclonal antibody was purchased from MBL. Rabbit anti-Flag monoclonal antibody was purchased from Sigma-Aldrich. Anti-HA was purchased from Roche. Mouse anti-phospho-histone H2AX (Ser139) antibody and Alexa Fluor 488 mouse anti-phospho-H3 (Ser10) antibody were purchased from Merck Millipore. Alexa Fluor 488 rabbit anti-mouse immunoglobulin (Ig)G, Alexa Fluor 488 goat anti-rabbit IgG and Alexa Fluor 555 goat anti-rabbit IgG were purchased from Invitrogen. TO-PRO3 was purchased from Molecular Probes. Rabbit anti-14-3-3 Sigma antibody was purchased from Bethyl laboratories. Sheep anti-c-TAK1 antibody was purchased from Exalpha Biologicals. Anti-sheep IgG-HRP was purchased from RSD. Nonviable cell exclusion was performed by 7-AAD Viability Staining Solution (BioLegend).

Subclone strategy and direct sequencing. Using genomic DNA of the patients as template, each targeted region was amplified by PCR with specific primers (Supplementary Table 4). PCR products were purified with illustra ExoStar (GE Healthcare) and subcloned into *Eco*RV site of pBluescript II KS(−) (Stratagene). Ligated plasmids were transformed into *E. coli* strain XL1-Blue by 45 s heat shock at 42 °C. Positive transformants were incubated on LB plates containing 100 μg ml^{-1} ampicillin supplemented with X-gal (Sigma-Aldrich) and isopropyl β-D-1-thiogalactopyranoside (Sigma-Aldrich). For colony PCR, a portion of a white colony was directly added to a PCR mixture as the DNA template. Insert region was amplified by PCR procedure with T3 and T7 universal primers, purified with illustra ExoStar (GE Healthcare Life Sciences), and sequenced by the Sanger method with T3 and T7 primers using BigDye Terminator v3.1 Cycle Sequencing kit (Applied Biosystems) and *ABI Prism 310* Genetic Analyzer (Life Technologies).

Immunoprecipitation and western blotting. These experiments were performed as described previously[30]. Briefly, HEK293T cells were transiently transfected with mammalian expression plasmids encoding Flag-tagged CDC25C and its mutants, HA-tagged 14-3-3 or c-TAK1. All plasmids were sequence verified. After 48 h, cell lysates were collected and incubated with an antibody (anti-HA antibody (1:200, 3 h), anti-Flag antibody (1:200, 3 h), anti-c-TAK1 antibody (1:150, 3 h) and anti 14-3-3 antibody (1:150, 3 h)). After incubation, the cell lysates were incubated with protein G-Sepharose (GE Healthcare) for 1 h. The precipitates were stringently washed with high salt-containing wash buffer and analysed by western blotting. Anti-Flag (HRP-conjugated, Sigma-Aldrich), anti-HA (MBL), anti-HA (HRP-conjugated, Roche), anti-CDC25C (Cell Signaling Technology), anti-phospho-CDC25C (Ser216) (Cell Signaling Technology), anti-c-TAK1 antibody (Exalpha Biologicals) or anti-14-3-3 antibody (Bethyl laboratories) antibodies and Immunostar LD (Wako) was used for detection. Original gel images of western blot analysis are shown in Supplementary Fig. 16.

Cell cycle synchronization and analysis for mitosis entry. After transduction of wild-type CDC25C or its mutated forms to murine lymphoid cell line Ba/F3 cells (RIKEN BioResource Center), double-thymidine block was performed to obtain cell cycle synchronization at G1/S phase. In brief, 2 mM of thymidine was added to the medium. After 16 h, cells were washed and released from the first thymidine for 8 h. A second block was initiated by adding 2 mM of thymidine, and cells were maintained for 16 h. Then thymidine was washed out and the cells were incubated with 1 mM nocodazole with or without 2 Gy of irradiation (Supplementary Fig. 10a). Ba/F3 cells were fixed over time with 75% ethanol in phosphate-buffered saline (PBS) at 4 °C overnight and permeabilized with 2% Triton-X at 4 °C for 15 min. The cells were stained with anti-phospho-H3 (Ser10) Alexa Fluor 488 conjugated antibody (dilution, 1:200) in PBS with 2% fetal calf serum at 4 °C for 30 min and then treated with 5% propidium iodide and 1% RNase in PBS at room temperature (RT) for 30 min. Cell cycle was analysed using a BD LSR II Flow cytometer (BD biosciences) (Supplementary Fig. 15b). To assess the cooperation of *CDC25C* and *RUNX1* mutation, wild-type or mutant (D234G, H437N) pMXs-neo-Flag-CDC25C and mutant (F303fsX566, R174X) pGCDNsam-IRES-KusabiraOrange-Flag-RUNX1 were retrovirally transduced into Ba/F3 cells.

Immunofluorescent microscopic analysis. These experiments were performed as described previously[30]. Briefly, Ba/F3 cells were fixed, permeabilized and blocked. Staining for phosphorylated histone H2AX was performed with anti-phospho-histone H2AX (Ser139) antibody (dilution, 1:500; Merck Millipore) at RT for 3 h. After washing with PBS three times and with 1% bovine serum albumin in PBS, the cells were treated with Alexa Fluor 488 rabbit anti-mouse IgG (dilution, 1:500; Invitrogen) and TO-PRO3 (dilution, 1:1,000; Molecular Probes) for 1 h. The proteins were visualized using FV10i (Olympus) or BZ-9000 (Keyence). The percentage of γH2AX foci-positive cells was determined by examining 100 cells per sample. Three independent experiments were performed. To evaluate the localization of CDC25C, Ba/F3 cells were treated with 2 mM thymidine for 12 h and stained. Staining was underwent with anti-Flag antibody or anti-CDC25C antibody at RT for 3 h. After washing, the cells were treated with Alexa Fluor 488 or 555 antibody and TO-PRO3 for 1 h. The mean intensity of CDC25C in the nucleus and cytoplasm of each cell was measured within a region of interest placed within the nucleus and cytoplasm (Supplementary Fig. 10). Similarly, the background intensity was quantified within the region of interest placed outside the cells. All the measurements were performed using the Fluoview FV10i software or ImageJ. The background-subtracted intensity ratio of the nucleus to cytoplasm was calculated in >30 cells in each specimen.

Retrovirus production. The procedures were performed as described previously[30]. Briefly, Plat-E packaging cells were transiently transfected with each retroviral construct using the calcium phosphate precipitation method, and supernatant

containing retrovirus was collected 48 h after transfection and used for infection after it was centrifuged overnight at 10,000 r.p.m.

Statistical analysis. To compare data between groups, unpaired Student's *t*-test was used when equal variance were met by the *F*-test. When unequal variances were detected, the Welch *t*-test was used. Differences were considered statistically significant at a P value of <0.05.

References

1. Song, W. J. *et al.* Haploinsufficiency of CBFA2 causes familial thrombocytopenia with propensity to develop acute myelogenous leukaemia. *Nat. Genet.* **23,** 166–175 (1999).
2. Ichikawa, M. *et al.* A role for RUNX1 in hematopoiesis and myeloid leukemia. *Int. J. Hematol.* **97,** 726–734 (2013).
3. Cameron, E. R. & Neil, J. C. The Runx genes: lineage-specific oncogenes and tumor suppressors. *Oncogene* **23,** 4308–4314 (2004).
4. Nickels, E. M., Soodalter, J., Churpek, J. E. & Godley, L. A. Recognizing familial myeloid leukemia in adults. *Ther. Adv. Hematol.* **4,** 254–269 (2013).
5. Liew, E. & Owen, C. Familial myelodysplastic syndromes: a review of the literature. *Haematologica* **96,** 1536–1542 (2011).
6. Kuramitsu, M. *et al.* Extensive gene deletions in Japanese patients with diamond-blackfan anemia. *Blood* **119,** 2376–2384 (2012).
7. Kirito, K. *et al.* A novel RUNX1 mutation in familial platelet disorder with propensity to develop myeloid malignancies. *Haematologica* **93,** 155–156 (2008).
8. Boutros, R., Lobjois, V. & Ducommun, B. CDC25 phosphatases in cancer cells: key players? Good targets? *Nat. Rev. Cancer* **7,** 495–507 (2007).
9. Kastan, M. B. & Bartek, J. Cell-cycle checkpoints and cancer. *Nature* **432,** 316–323 (2004).
10. Peng, C. Y. *et al.* C-TAK1 protein kinase phosphorylates human Cdc25C on serine 216 and promotes 14-3-3 protein binding. *Cell Growth Differ.* **9,** 197–208 (1998).
11. Lopez-girona, A., Furnari, B., Mondesert, O. & Early, P. R. Nuclear localization of Cdc25 is regulated by DNA damage and a 14-3-3 protein. *Nature* **397,** 172–175 (1999).
12. Satoh, Y., Matsumura, I., Tanaka, H. & Harada, H. C-terminal mutation of RUNX1 attenuates the DNA-damage repair response in hematopoietic stem cells. *Leukemia* **26,** 303–311 (2011).
13. Krejci, O. *et al.* p53 signaling in response to increased DNA damage sensitizes AML1-ETO cells to stress-induced death. *Blood* **111,** 2190–2199 (2008).
14. Park, J. *et al.* Mutation profiling of mismatch repair-deficient colorectal cancers using an in silico genome scan to identify coding microsatellites advances in brief mutation profiling of mismatch repair-deficient colorectal cancers using an in silico genome scan to Ide. *Cancer Res.* **62,** 1284–1288 (2002).
15. Vassileva, V., Millar, A., Briollais, L., Chapman, W. & Bapat, B. Genes involved in DNA repair are mutational targets in endometrial cancers with microsatellite instability. *Cancer Res.* **62,** 4095–4099 (2002).
16. Greif, P. A. *et al.* GATA2 zinc finger 1 mutations associated with biallelic CEBPA mutations define a unique genetic entity of acute myeloid leukemia. *Blood* **120,** 395–403 (2012).
17. Ostergaard, P. *et al.* Mutations in GATA2 cause primary lymphedema associated with a predisposition to acute myeloid leukemia (Emberger syndrome). *Nat. Genet.* **43,** 929–931 (2011).
18. Hahn, C. N. *et al.* Heritable GATA2 mutations associated with familial myelodysplastic syndrome and acute myeloid leukemia. *Nat Genet.* **43,** 1012–1017 (2011).
19. Hsu, A. P. *et al.* Mutations in GATA2 are associated with the autosomal dominant and sporadic monocytopenia and mycobacterial infection (MonoMAC) syndrome. *Blood* **118,** 2653–2655 (2011).
20. Dickinson, R. E. *et al.* Exome sequencing identifies GATA-2 mutation as the cause of dendritic cell, monocyte, B and NK lymphoid deficiency. *Blood* **118,** 2656–2658 (2011).
21. Zhang, S.-J. *et al.* Gain-of-function mutation of GATA-2 in acute myeloid transformation of chronic myeloid leukemia. *Proc. Natl Acad. Sci. USA* **105,** 2076–2081 (2008).
22. Hasegawa, D. *et al.* CBL mutation in chronic myelomonocytic leukemia secondary to familial platelet disorder with propensity to develop acute myeloid leukemia (FPD/AML). *Blood* **119,** 2612–2614 (2012).
23. Turowski, P. *et al.* Functional cdc25C dual-specificity phosphatase is required for S-phase entry in human cells. *Mol. Biol. Cell* **14,** 2984–2998 (2003).
24. Michaud, J. *et al.* In vitro analyses of known and novel RUNX1/AML1 mutations in dominant familial platelet disorder with predisposition to acute myelogenous leukemia: Implications for mechanisms of pathogenesis. *Blood* **99,** 1364–1372 (2002).
25. Kohlmann, A. *et al.* Monitoring of residual disease by next-generation deep-sequencing of RUNX1 mutations can identify acute myeloid leukemia patients with resistant disease. *Leukemia* **28,** 129–137 (2014).
26. Chen, C. Y. *et al.* RUNX1 gene mutation in primary myelodysplastic syndrome - The mutation can be detected early at diagnosis or acquired during disease progression and is associated with poor outcome. *Br. J. Haematol.* **139,** 405–414 (2007).
27. Sakurai, M. *et al.* Impaired hematopoietic differentiation of RUNX1-mutated induced pluripotent stem cells derived from FPD/AML patients. *Leukemia.* (epub ahead of print 15 April 2014; doi:10.1038/leu.2014.136).
28. Bravo, J., Li, Z., Speck, N. A. & Warren, A. J. The leukemia-associated AML1 (Runx1)-CBF beta complex functions as a DNA-induced molecular clamp. *Nat. Struct. Biol.* **8,** 371–378 (2001).
29. Akamatsu, Y., Tsukumo, S. I., Kagoshima, H., Tsurushita, N. & Shigesada, K. A simple screening for mutant DNA binding proteins: application to murine transcription factor PEBP2?? subunit, a founding member of the Runt domain protein family. *Gene* **185,** 111–117 (1997).
30. Yoshimi, A. *et al.* Evi1 represses PTEN expression and activates PI3K/AKT/mTOR via interactions with polycomb proteins. *Blood* **117,** 3617–3628 (2011).

Acknowledgements

This work was supported in part by grants-in-aid from the Ministry of Health, Labor and Welfare of Japan (H23-Nanchi-Ippan-104; M. Kurokawa) and KAKENHI (24659457; M. Kurokawa). We thank R. Lewis (University of Nebraska Medical Center) and T. Kitamura (Institute of Medical Science, The University of Tokyo) for providing essential materials; T. Koike (Nagaoka Red Cross Hospital), K. Nara (Ootemachi Hospital), K. Suzuki (Japanese Red Cross Medical Center), H. Harada (Fujigaoka Hospital), Y. Morita (Kinki University), M. Matsuda (PL Hospital), H. Kashiwagi (Osaka University), T. Kiguchi (Chugoku Central Hospital), T. Masunari (Chugoku Central Hospital), K. Yamamoto (Yokohama City Minato Red Cross Hospital), T. Takahashi (Mitsui Memorial Hospital) and T. Takaku (Juntendo University) for providing patient samples; M. Kuramitsu (National Institutte of Infectious Diseases) for providing kind support of synchronized quantitative PCR; and K. Tanaka and Y. Shimamura for their technical assistance.

Author contributions

A.Y., T.T., M.I. and M. Kurokawa analysed genetic materials and performed functional studies. A.T., H.I., M.N., Y.N. and S.A. were involved in sequencing and/or functional studies. M. Kawazu, T.U. and H.M. took part in whole-exome sequencing, deep sequencing and bioinformatics analyses of the data. A.Y., T.T., M.I., H.H., K.U., Y.H., E.I., K.K. and H.N. collected specimens. A.Y. and T.T. generated figures and tables. M. Kurokawa designed and led the entire project. A.Y., T.T. and M. Kurokawa wrote the manuscript. All authors participated in the discussion and interpretation of the data.

Additional information

Accession codes: Sequence data for FPD/AML patients has been deposited in GenBank/EMBL/DDBJ sequence read archive (SRA) under the accession code SRP043031

Supplementary Information accompanies this paper at http://www.nature.com/naturecommunications

Competing financial interests: The authors declare no competing financial interests.

Reprints and permission information is available online at http://npg.nature.com/reprintsandpermissions

How to cite this article: Yoshimi, A. *et al.* Recurrent *CDC25C* mutations drive malignant transformation in FPD/AML. *Nat. Commun.* 5:4770 doi: 10.1038/ncomms5770 (2014).

Original Article
EPIDEMIOLOGY/GENETICS

Obesity

Successfully Achieving Target Weight Loss Influences Subsequent Maintenance of Lower Weight and Dropout From Treatment

Tomohide Yamada, Kazuo Hara, Akiko Kishi Svensson, Nobuhiro Shojima, Jun Hosoe, Minaka Iwasaki, Toshimasa Yamauchi, and Takashi Kadowaki

Objectives: The influence of the amount and rate of weight loss on subsequently regaining weight and dropout from treatment in severely obese patients targeting 5% weight loss was investigated.

Methods: A total of 120 consecutive hospital patients with severe obesity (BMI: 42 ± 9 kg/m^2) participated in an inpatient program targeting 5% weight loss that involved goal setting, charting weight four times daily, and diet and exercise. They were followed after discharge to assess subsequent regaining of weight and dropout.

Results: Mean weight loss was 4.9 ± 2.4% after a mean of 19 days in the hospital, and 43% of the patients achieved the target weight loss (>5%). Over the median 2-year follow-up period, greater than 5% in-hospital weight loss was associated with a significantly lower risk of regaining weight after adjustment for various factors (>5% to ≤7% loss: hazard ratio 0.30 [0.11-0.85] for regaining all of the lost weight and 0.32 [0.13-0.78] for regaining half of the lost weight). No significant relation between the amount or rate of weight loss and dropout from subsequent outpatient treatment was seen.

Conclusions: Successfully achieving the target weight loss in a comprehensive program predicts subsequent maintenance of lower weight without increasing the risk of dropout. Successful in-hospital weight loss might increase the motivation of obese patients.

Obesity (2015) **23**, 183–191. doi:10.1002/oby.20874

Introduction

Obesity has rapidly become a worldwide epidemic (1) and it is a major risk factor for various disorders (2). Obesity and type 2 diabetes both increase the risk of cardiovascular disease and other comorbidities (3). A J-shaped relationship between body mass index (BMI) and average life expectancy was demonstrated by a study of 1.46 million white adults (4). Among non-smoking Caucasian males and females in the United States, the relative risk of death after 10 years was lowest for those with a BMI of 22.5-24.9 (reference hazard ratio [HR] of 1.0), but the risk increased along with BMI. Thus, the HR was 1.44 for both women and men with a BMI of 30-34.9 (obesity class I), 1.88 for women and 2.06 for men with a BMI of 35-39.9 (obesity class II), and 2.51 for women and 2.93 for men with a BMI of 40-49.9 (obesity class III). Therefore, it is important to treat severe obesity, which markedly increases the risk of death.

Even modest weight loss (3%-5% of body weight) can result in clinically meaningful benefits with respect to reducing triglycerides, blood glucose, and glycated hemoglobin, as well as decreasing the risk of type 2 diabetes, while greater weight loss (>5%) reduces blood pressure, further improves the lipid profile (both low-density and high-density lipoprotein cholesterol), and decreases the need for medications to control blood pressure, blood glucose, and lipids (5).

Although many obese people successfully lose weight by dieting and/or behavioral therapy (using their own methods or whatever is popular at the time), most of them subsequently regain the weight that they lost. Accordingly, new strategies are required to reduce weight and maintain weight loss. Bariatric surgery can be a highly effective option for adults with a BMI greater than 35 kg/m^2 and type 2 diabetes, especially if diabetes or associated comorbidities are difficult to control by lifestyle modification and pharmacotherapy (3). However, such surgery has not become popular in Japan for reasons related to the technique and indications (6). According to the OECD report published in 2014, the rate of obesity (BMI > 30) among Japanese adults is only 3.6%, which is one

Department of Diabetes and Metabolic Diseases, Graduate School of Medicine, University of Tokyo, Japan. Correspondence: Kazuo Hara (haratky@gmail.com)

Disclosure: The authors declared no conflict of interest.

Author contributions: T. Yamada., K.H., and T.K. conceived the idea of the study and were responsible for the design of the study. T. Yamada and K.H. were responsible for undertaking the data analysis and produced the tables and figures. T. Yamada and K.H. provided input into the data analysis. The initial draft of the manuscript was prepared by T. Yamada and K.H. and then circulated repeatedly among all authors for critical revision. T. Yamada was responsible for acquisition of the data, and T. Yamada, K.H., N.S., A.K.S., J.H., M.I., T. Yamauchi, and T.K. contributed to interpretation of the results.

Additional Supporting Information may be found in the online version of this article.

Received: 5 June 2014; **Accepted:** 1 August 2014; **Published online 16 October 2014. doi:10.1002/oby.20874**

quarter of that in Germany (14.7%) and one tenth of that in the United States (35.3%) (7).

A recent systematic review and meta-analysis (8) showed that behavioral interventions dealing with both diet and physical activity provide a small, but significant, benefit for the maintenance of weight loss. However, little is known about the optimal amount and rate of weight loss for preventing subsequent weight gain and dropout from weight loss programs in patients with obesity and diabetes, although a few studies have shown that initial achievement of weight loss is related to better adherence and success with maintaining a lower weight (9,10). Initiation or intensification of insulin or sulfonylurea therapy commonly results in weight gain in patients with type 1 or type 2 diabetes (11,12). In addition, it was recently reported that antidepressant therapy increases the risk of regaining weight in overweight individuals with impaired glucose tolerance (13).

Clarifying the relationship between weight loss and regaining weight or dropout from weight loss programs is useful to explore more effective new strategies for obesity. In the present study, we assessed the influence of inpatient weight loss on the risk of subsequently regaining weight and dropout from treatment among patients with severe obesity who completed a comprehensive weight loss education program and did not receive bariatric surgery.

Methods

Subjects

First, we screened 2,178 consecutive patients who were admitted to the University of Tokyo Hospital between 2009 and 2012. Among them, we selected patients with severe obesity who had a BMI $\geq$35 kg/m^2 and who participated in a comprehensive weight loss program. We excluded patients with severe cardiovascular disease, heart failure, infectious diseases, stroke, or peripheral artery disease, as well as patients with type 1 diabetes, pregnant women, patients with dementia, patients who had orthopedic diseases that could interfere with exercise (walking), perioperative patients, patients taking anti-obesity medications, patients who had undergone bariatric surgery, patients without pertinent data, patients who were transferred to another hospital immediately after discharge, patients who were readmitted, and those under 18 or over 80 years old. The remaining patients were followed after discharge to assess subsequent weight gain and dropout.

Comprehensive inpatient obesity treatment program targeting 5% weight loss

The details of this program have been reported previously (14). Briefly, it consisted of three main components, which were behavioral modification (goal setting and charting weight four times daily), diet, and exercise (patients with diabetes received appropriate anti-diabetic therapy together with this weight loss program, and the treatment of diabetes was decided by each attending physician).

Behavioral modification (goal setting and charting weight four times daily)

At admission, all patients were given the goal of achieving 5% weight loss while in the hospital. They also weighed themselves four times daily (immediately after waking, immediately after breakfast, immediately after dinner, and immediately before going to bed) and charting the data on a weekly graph. Daily charting of weight fluctuations reveals irregular intake of food and fluid that reflects dysfunctional eating patterns and other behavioral abnormalities, and assists in achieving weight loss (15,16). Patients were recommended to continue charting their weight after discharge. Patients were weighed by using AD-6107NW^{TM} scales (A and D Co. Ltd., Tokyo, Japan).

Diet

A balanced low-calorie diet (20-24 kcal/day/kg of ideal body weight, e.g., the diet for a person with a height of 1.7 m would be calculated for the ideal body weight based on a BMI of 22 as ($1.7 \times 1.7 \times 22 = 63.58$ kg) $\times 20 = 1{,}271$ kcal or $\times 24 = 1{,}525$ kcal) was provided to the patients in the hospital, consisting of 50%-60% carbohydrate, 20% protein, and 20%-30% fat. Hospital dietitians used food samples and a food exchange table (17) to educate patients about nutritional guidelines. The dietician initially gave each patient information for 1 hour, with subsequent 30-minutes sessions being held at least twice a week until discharge.

Exercise

All patients were given a pedometer and were instructed to walk more than 10,000 steps/daily (a distance of 5-7 km) over approximately 1.5 hours. Using a map of the University of Tokyo Hospital (site area: 540,000 m^2), each patient marked out a route around the hospital compound and walked it as part of their regular exercise routine. The exercise program was tailored to accommodate health problems (e.g., morbid obesity, hypoglycemia, joint pain, or diabetic retinopathy) and specific needs (e.g., exercise by walking or training on a bicycle ergometer). The target pulse rate and schedule for each exercise session were set.

Outcome measures

Patients attended our hospital outpatient department every 2 months after discharge to continue their weight loss program and for treatment of other diseases (diabetes, dyslipidemia, and hypertension). Body weight was measured at each visit. The outcomes of this study were regaining weight and dropout from the weight loss program after discharge. Regaining all of the lost weight (100% regain) was defined as returning to the baseline body weight at the time of admission. Regaining half of the lost weight (50% regain) was defined as returning to a body weight midway between that at admission and that at discharge, while 25% and 75% regain were defined similarly. Dropout from the program was defined as missing outpatient appointments. (If the patient presented again within 6 months of the specified appointment, this was not defined as dropout.) Patients were defined as having diabetes if the medical record listed a diagnosis of type 2 diabetes and they were using oral hypoglycemic agents and/or insulin. If a 75-g oral glucose tolerance test was performed, a diagnosis of diabetes, impaired glucose tolerance, or impaired fasting glucose was made according to the American Diabetes Association criteria (18).

Antidepressant medications were classified as selective serotonin reuptake inhibitors, serotonin and norepinephrine reuptake inhibitors, tricyclic antidepressants, tetracyclic antidepressants, serotonin

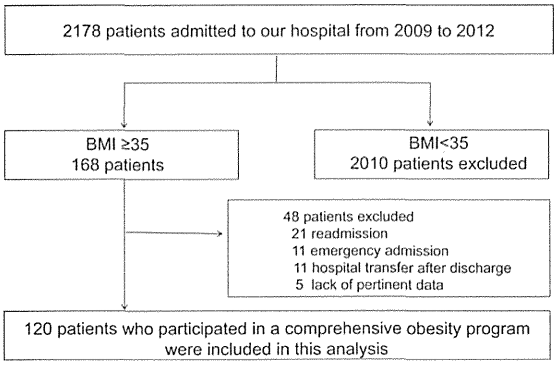

Figure 1 Flow chart of patient disposition.

receptor antagonists and reuptake inhibitors, monoamine oxidase inhibitors, and noradrenergic and specific serotonergic antidepressants. All demographic and clinical data were collected from secure electric medical records. The accuracy of the body weight measurements of each subject was confirmed by nurses or physicians.

Statistical analysis

Continuous variables are presented as the mean ± SD. The chi-square test, t-test, or ANOVA was used to assess differences among weight loss categories (≤3% loss; >3% to ≤5% loss; >5% to ≤7% loss; >7% loss), quartiles of weight loss achieved (%) during hospitalization, or the rapidity of weight loss after admission (rapid loss was defined as >3% loss within 7 days after admission and non-rapid loss was ≤3% loss after 7 days) among patients who achieved greater than 3% weight loss during hospitalization. Multivariate regression analysis using the Cox proportional hazards model was employed to determine the adjusted HR and 95% confidence interval (CI) for regaining weight, dropout in relation to the duration of hospitalization, age, sex, BMI, smoking, type 2 diabetes, insulin therapy, sulfonylurea therapy, antidepressant medication, and hospital diet (calories per day). We used STATA statistical software version 12.0 for all analyses. All P values were two-sided and significance was accepted at $P < 0.05$. This retrospective cohort study complied with the Declaration of Helsinki and it was approved by the Research Ethics Committee of the University of Tokyo Hospital.

Results

Patient selection

Figure 1 is a flow chart showing the disposition of the patients. A total of 2,178 consecutive adults with severe obesity were admitted to our hospital between January 2009 and December 2012. Among them, 2,010 were excluded because their BMI was less than 35 kg/m^2. Among the remaining 168 patients, 48 were excluded (21 because of readmission to our department to treat diabetes and obesity, 11 due to emergency admission, 11 due to transfer to another hospital immediately after discharge, and 5 for lack of pertinent data). The remaining 120 patients were included in this study.

Baseline characteristics

Table 1 shows the baseline characteristics of the subjects. They had a mean age of 48 ± 14 years, a mean BMI of 41.7 ± 8.8 kg/m^2, and 58% were women. In addition, 74% had diabetes, 21% had impaired glucose tolerance and/or impaired fasting glucose, and the mean HbA_{1c} was 7.6 ± 2.2%. After a mean of 19 days (19 ± 10) in the hospital, the mean weight loss was 4.9 ± 2.4% (5.3 ± 3.0 kg) and 43% of the patients achieved the target weight loss of greater than 5%. There were no significant differences of these parameters

TABLE 1 Baseline characteristics of groups stratified by the extent of weight loss during hospitalization (≤3% loss; >3% to ≤5% loss; >5% to ≤7% loss; >7% loss)

		Extent of weight loss				
Variable	All subjects	≤3% loss	>3% to ≤5% loss	>5% to ≤7% loss	>7% loss	*P* value
N	120	20 (17)	48 (40)	35 (29)	17 (14)	
Sex (female)	69 (58)	12 (60)	24 (50)	23 (66)	10 (59)	0.55
Age (years)	48 ± 14	46 ± 18	48 ± 13	50 ± 13	47 ± 12	0.76
Body weight (kg)	109 ± 22	103 ± 25	110 ± 23	107 ± 19	114 ± 22	0.42
Height (cm)	162 ± 10	162 ± 11	163 ± 10	160 ± 9	163 ± 8	0.65
BMI (kg/m^2)	42 ± 9	39 ± 6	41 ± 6	44 ± 13	43 ± 7	0.19
Waist circumference (cm)	125 ± 15	121 ± 15	125 ± 15	124 ± 13	130 ± 18	0.28
Current smoker	49 (41)	9 (45)	20 (42)	12 (34)	8 (47)	0.79
Type 2 diabetes	89 (74)	17 (85)	38 (79)	23 (66)	11 (65)	0.27
Insulin use	25 (21)	7 (35)	9 (19)	7 (20)	2 (12)	0.33
Sulfonylurea use	9 (8)	2 (10)	3 (6)	2 (6)	2 (12)	0.83
Hospital diet (kcal/day/kg of ideal body weight)	22.6 (2.4)	22.8 (2.3)	22.8 (2.8)	22.7 (1.9)	21.8 (1.9)	0.50
Antidepressant use	18 (15)	2 (10)	6 (13)	7 (20)	3 (18)	0.70

Data are the mean ± SD or number (%). BMI, body mass index.

TABLE 2 Baseline characteristics of groups stratified by the rapidity of weight loss after admission

Variable	All	Rapidity of weight loss		*P* value
		Non-rapid loss (≤3% loss within 7 days)	Rapid loss (>3% loss within 7 days)	
N	100	39 (39)	69 (69)	
Sex (female)	57 (57)	22 (56)	35 (57)	0.92
Age (years)	49 ± 13	49 ± 13	49 ± 14	0.98
Body weight (kg)	110 ± 22	109 ± 21	111 ± 22	0.68
Height (cm)	162 ± 9	161 ± 9	163 ± 10	0.40
BMI (kg/m^2)	43 ± 9	44 ± 12	42 ± 6	0.23
Waist circumference (cm)	125 ± 15	124 ± 16	126 ± 14	0.44
Current smoker	40 (40)	15 (38)	25 (41)	0.80
Type 2 diabetes	72 (72)	29 (74)	43 (70)	0.67
Insulin use	18 (18)	6 (15)	12 (20)	0.59
Sulfonylurea use	7 (7)	5 (13)	2 (3)	0.07
Hospital diet (kcal/day/kg of ideal body weight)	22.6 (2.4)	22.6 (2.4)	22.6 (2.4)	0.93
Antidepressant use	16 (16)	7 (18)	9 (15)	0.67

Data are the mean ± SD or number (%). BMI, body mass index.
Rapid loss group: patients who achieved >3% weight loss within 7 days after admission among patients with >3% weight loss during hospitalization. Non-rapid loss group: patients who achieved ≤3% weight loss within 7 days after admission.

among groups stratified by the extent of weight loss (≤3% loss; >3% to ≤5% loss; >5% to ≤7% loss; >7% loss) (Table 1). There were also no significant differences among patients stratified into quartiles based on weight loss achieved (%) during hospitalization (Table S1). Furthermore, there were no differences between two groups based on the rapidity of weight loss after admission (>3% loss within 7 days vs. ≤3% loss) (Table 2).

Risk of weight regain and dropout from treatment after discharge in relation to percent weight loss during hospitalization

Over the median follow-up period of 1.8 years (1.8 ± 1.1 years) after discharge, 32 of the 120 patients (27%) regained all of the weight they had lost (100% regain), 54 patients (45%) regained half of the weight they had lost (50% regain), and 32 patients (27%) dropped out of the program (Table 3). Multivariate regression analysis using the Cox proportional hazards model showed that greater than 5% weight loss was associated with a significantly lower risk of regaining all of the lost weight (100% regain) compared with ≤3% weight loss after adjustment for the duration of hospitalization, age, sex, BMI, smoking, diabetes, use of insulin, sulfonylureas, and antidepressants, and hospital diet (calories) (>7% loss: HR 0.04 [0.004-0.37, $P = 0.005$]; 5% to ≤7% loss: HR 0.3 [0.11-0.85, $P = 0.02$]). In addition, greater than 3% weight loss was associated with a significantly lower risk of regaining half of the lost weight (50% regain) (>7% loss: HR 0.18 [0.05-0.59, $P = 0.005$]; 5% to ≤7% loss: HR 0.32 [0.13-0.78, $P = 0.01$]; 3% to ≤5% loss: HR 0.41 [0.19-0.92, $P = 0.03$]). Analysis of the risk of 25% or 75% regain yielded similar results. There was no significant relation between the extent of weight loss and dropout from treatment (Table 3, Figure 2, Figure S1).

Risk of weight regain and dropout from treatment after discharge in relation to weight loss quartiles

We also performed an analysis of the subjects stratified by quartiles of weight loss achieved during hospitalization (Table S2, Figure 3, Figure S2). The highest weight loss quartile (quartile 4) had a significantly lower risk of regaining all of the weight (100% regain) compared with the lowest quartile (quartile 1) after adjustment for various covariates (HR 0.14 [0.04-0.54], $P = 0.004$ for 100% regain; HR 0.22 [0.08-0.65], $P = 0.006$ for 75% regain; HR 0.27 [0.1-0.69], $P = 0.007$ for 50% regain; and HR 0.37 [0.15-0.93], $P = 0.03$ for 25% regain).

Rapidity of weight loss versus the risk of weight regain and dropout

Among patients who achieved greater than 3% weight loss during hospitalization ($N = 100$), adjusted analysis showed that rapid weight loss (>3% within 7 days after admission) did not significantly increase the risk of subsequently regaining weight compared with patients who showed slower weight loss (≤3% within 7 days) (HR 1.1 [0.43-2.85], $P = 0.84$ for regaining all of the lost weight [100% regained], HR 1.11 [0.55-2.25], $P = 0.77$ for regaining half of the lost weight [50% regained]) (Table 4, Figure 4).

Discussion

The present study indicated that achieving greater than 5% initial weight loss (the target) during comparatively brief hospitalization was an independent predictor of subsequent maintenance of lower

TABLE 3 Multivariate regression analysis with the Cox proportional hazards model assessing risk factors for regaining weight and dropout after discharge in patients stratified by weight loss (%) during hospitalization

No of event/ *N* Variable	Regaining all of the weight lost (100% regain) 32/120 (27%)		Regaining three quarters of the weight lost (75% regain) 45/120 (38%)		Regaining half of the weight lost (50% regain) 54/120 (45%)		Regaining one quarter of the weight lost (25% regain) 58/120 (48%)		Dropout from outpatient treatment 32/120 (27%)	
	Multivariate	*P*	Multivariate	*P*	Multivariate	*P*	Multivariate	*P*	Multivariate	*P*
Sex (female)	1.51 (0.61-3.78)	0.38	0.75 (0.35-1.60)	0.45	0.99 (0.49-1.98)	0.97	0.93 (0.48-1.81)	0.83	1.16 (0.51-2.62)	0.73
Age (years)	0.98 (0.95-1.00)	0.09	0.99 (0.97-1.02)	0.64	1.00 (0.97-1.02)	0.82	1.00 (0.97-1.02)	0.74	0.97 (0.94-1.00)	0.07
BMI (kg/m^2)	0.98 (0.92-1.04)	0.46	0.99 (0.95-1.04)	0.78	1.01 (0.97-1.05)	0.75	0.99 (0.95-1.04)	0.68	1.00 0.94-1.05)	0.89
Current smoker	1.41 (0.58-3.42)	0.44	1.15 (0.56-2.35)	0.70	0.96 (0.50-1.84)	0.90	1.02 (0.55-1.89)	0.94	0.84 (0.38-1.85)	0.67
Type 2 diabetes	0.82 (0.30-2.23)	0.69	1.37 (0.57-3.28)	0.48	1.36 (0.59-3.12)	0.48	1.34 (0.61-2.96)	0.47	0.44 (0.19-1.06)	0.07
Duration of hospital stay (days)	1.03 (0.98-1.08)	0.26	1.04 (1.00-1.08)	0.05	1.03 (0.99-1.06)	0.11	1.02 (0.99-1.06)	0.15	1.01 (0.97-1.06)	0.59
Insulin use	0.94 (0.34-2.57)	0.90	0.80 (0.34-1.86)	0.60	1.11 (0.51-2.42)	0.79	1.26 (0.61-2.58)	0.53	0.76 (0.22-2.59)	0.66
Sulfonylurea use	1.92 (0.36-10.1)	0.44	1.04 (0.27-3.97)	0.96	1.94 (0.64-5.92)	0.24	1.9 (0.65-5.61)	0.24	0.77 (0.09-6.50)	0.81
Antidepressant use	0.91 (0.29-2.83)	0.87	1.33 (0.50-3.51)	0.57	1.73 (0.73-4.12)	0.22	2.23 (1.03-4.82)	0.04	1.21 (0.46-3.23)	0.70
Hospital diet (kcal/day/kg of ideal body weight)	1.04 (0.87-1.24)	0.67	1.09 (0.94-1.27)	0.25	1.1 (0.97-1.25)	0.14	1.07 (0.95-1.21)	0.28	1.03 (0.89-1.19)	0.71
Extent of weight loss										
≤3%	1.00	-	1.00	-	1.00	-	1.00	-	1.00	-
>3% to ≤5%	0.45 (0.18-1.15)	0.09	**0.36 (0.15-0.85)**	**0.02**	**0.41 (0.19-0.92)**	**0.03**	0.47 (0.22-1.01)	0.05	1.36 (0.48-3.85)	0.56
>5% to ≤7%	**0.30 (0.11-0.85)**	**0.02**	**0.38 (0.15-0.96)**	**0.04**	**0.32 (0.13-0.78)**	**0.01**	**0.37 (0.15-0.89)**	**0.03**	0.51 (0.15-1.7)	0.28
>7%	**0.04 (0.004-0.37)**	**0.005**	**0.08 (0.02-0.4)**	**0.002**	**0.18 (0.05-0.59)**	**0.005**	**0.29 (0.09-0.92)**	**0.04**	0.51 (0.12-2.18)	0.36

Data are the mean ± SD or number (%). BMI, body mass index. Cox proportional hazards analysis was employed to identify parameters significantly associated with weight gain and dropout from treatment after discharge using the following factors: duration of hospitalization, sex, age, BMI, current smoking, type 2 diabetes, insulin use, sulfonylurea use, antidepressant use, hospital diet (kcal/day/kg of ideal body weight), and extent of weight loss during hospitalization (≤3%, >3% to ≤5%, >5% to ≤7%, and >7%).
Bold values represents a statistical significant hazard ratio and p value ($p < 0.05$).

TABLE 4 Multivariate regression analysis with the Cox proportional hazards model assessing risk factors for regaining weight and dropout after discharge in patients stratified by rapidity of weight loss during hospitalization

No. of event/ *N* Variable	Regaining all of the weight lost (100% regain) 21/100 (21%)		Regaining three quarters of the weight lost (75% regain) 33/100 (33%)		Regaining half of the weight lost (50% regain) 40/100 (43%)		Regaining one quarter of the weight lost (25% regain) 43/100 (43%)		Dropout from outpatient treatment 26/100 (26%)	
	Multivariate	*P*	Multivariate	*P*	Multivariate	*P*	Multivariate	*P*	Multivariate	*P*
Sex (female)	2.60 (0.82-8.29)	0.11	0.87 (0.36-2.10)	0.76	1.06 (0.47-2.37)	0.89	1.09 (0.50-2.35)	0.83	1.36 (0.58-3.15)	0.48
Age (years)	0.96 (0.92-1.00)	0.08	0.98 (0.95-1.02)	0.32	0.98 (0.95-1.01)	0.30	0.98 (0.95-1.01)	0.29	0.98 (0.95-1.02)	0.28
BMI (kg/m^2)	1.00 (0.94-1.08)	0.90	1.01 (0.95-1.07)	0.80	1.01 (0.96-1.07)	0.60	0.99 (0.94-1.05)	0.72	1.00 (0.94-1.06)	0.98
Current smoker	1.43 (0.55-3.69)	0.47	1.15 (0.53-2.53)	0.72	1.01 (0.49-2.08)	0.98	1.14 (0.58-2.21)	0.71	1.08 (0.46-2.56)	0.86
Type 2 diabetes	1.27 (0.39-4.17)	0.69	2.08 (0.76-5.66)	0.15	1.96 (0.77-4.97)	0.16	1.71 (0.72-4.09)	0.22	0.44 (0.18-1.06)	0.07
Duration of hospital stay (days)	0.99 (0.94-1.03)	0.59	1.01 (0.97-1.04)	0.70	1.01 (0.96-1.04)	0.66	1.01 (0.98-1.04)	0.50	0.98 (0.93-1.03)	0.42
Insulin use	0.52 (0.12-2.21)	0.38	0.53 (0.17-1.66)	0.28	0.87 (0.33-2.28)	0.78	1.03 (0.42-2.51)	0.94	0.24 (0.03-1.95)	0.18
Sulfonylurea use	2.34 (0.36-15.4)	0.38	1.22 (0.28-5.36)	0.79	1.90 (0.51-7.07)	0.34	1.84 (0.50-6.76)	0.36	0.86 (0.10-7.62)	0.89
Antidepressant use	0.82 (0.24-2.78)	0.75	1.45 (0.52-4.03)	0.48	1.59 (0.62-4.09)	0.33	2.24 (0.98-5.12)	0.06	1.16 (0.41-3.28)	0.78
Hospital diet (kcal/day/kg of ideal body weight)	1.19 (0.98-1.44)	0.07	1.17 (1.00-1.37)	0.05	1.16 (1.01-1.33)	0.04	1.14 (0.99-1.31)	0.07	0.96 (0.80-1.15)	0.65
Rapidity of weight loss										
Non-rapid loss (≤3% loss within 7 days)	1.00	-	1.00	-	1.00	-	1.00	-	1.00	-
Rapid loss (>3% loss within 7 days)	1.11 (0.43-2.85)	0.84	1.08 (0.50-2.33)	0.85	1.11 (0.55-2.25)	0.77	1.26 (0.64-2.48)	0.51	1.21 (0.51-2.85)	0.67

Data are the mean ± SD or number (%). BMI, body mass index. Cox proportional hazards analysis was employed to identify parameters significantly associated with weight gain and dropout from treatment after discharge using the following factors: duration of hospitalization, sex, age, BMI, current smoking, type 2 diabetes, insulin use, sulfonylurea use, antidepressant use, hospital diet (kcal/day/kg of ideal body weight), and the rapidity of weight loss after admission. Rapid loss group: patients who achieved >3% weight loss within 7 days of admission among patients with >3% weight loss during hospitalization. Non-rapid loss group: patients who achieved ≤3% loss within 7 days of admission.

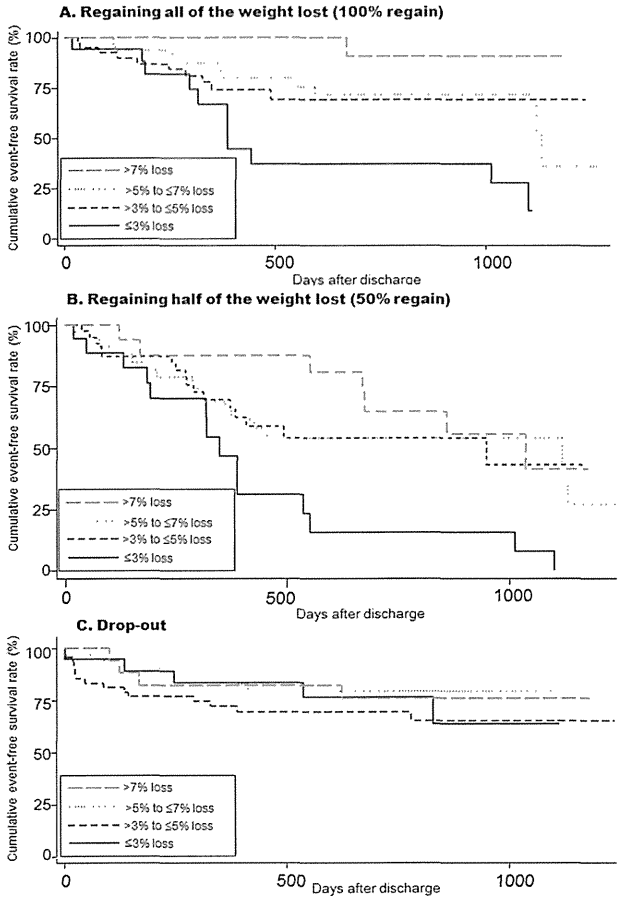

Figure 2 Kaplan–Meier curves for (A) regaining all of the weight lost (100% regain), (B) regaining half of the weight lost (50% regain), and (C) dropout from treatment after discharge in patients with severe obesity stratified by weight loss (%) during hospitalization. [Color figure can be viewed in the online issue, which is available at wileyonlinelibrary.com.]

weight by severely obese patients who completed a comprehensive program that involved behavioral modification (charting weight four times daily), even after adjustment for other covariates such as BMI and baseline drug therapy, without increasing the risk of dropout from treatment. Thus, a short-term intensive inpatient program targeting 5% weight loss may be clinically useful for achieving long-term improvement of weight. The 5% target we employed is consistent with the recent AHA/ACC/TOS Guidelines for Managing Overweight and Obesity in Adults (5), which states that greater than 5% weight loss can reduce blood pressure, improve the lipid profile and reduce the use of medications for hypertension, hyperglycemia, and hyperlipidemia in obese adults with cardiovascular risk factors. In addition, even modest weight loss (3%-5% of body weight) is beneficial with regard to improving the levels of triglycerides, blood glucose, and glycated hemoglobin, as well as reducing the risk of type 2 diabetes. Moreover, we showed that rapid weight loss did not significantly increase the risk of subsequently regaining weight and there was no significant relation between the pattern of weight loss (both its extent and rapidity) and dropout from treatment after adjustment for several covariates.

There were two novel elements of our weight loss program. First, the participants were each set a precise weight loss goal (5%) at the time of admission to motivate them. Second, we used charting weight four times daily as a behavioral modification technique (15,16). The goal setting theory was developed by Locke et al. (19). Goals are a form of motivation in which standards for self-satisfaction with performance are specified. Setting goals can influence the outcome in four ways. (a) Choice: goals focus attention and direct efforts to goal-related activities and away from perceived undesirable and irrelevant actions. (b) Effort: goals can lead to more effort. (c) Persistence: people are more likely to persevere despite setbacks if they are pursuing a goal. (d) Cognition: goals can lead individuals to change their behavior. Frequent self-weighing has previously been suggested to improve self-regulation of behavior (20). It probably assists in maintaining weight loss because frequent charting of weight fluctuations reveals irregular dietary habits that reflect other behavioral abnormalities. Once these irregularities become apparent to patients, they tend to improve their eating habits and/or lifestyle, which assists in progress with

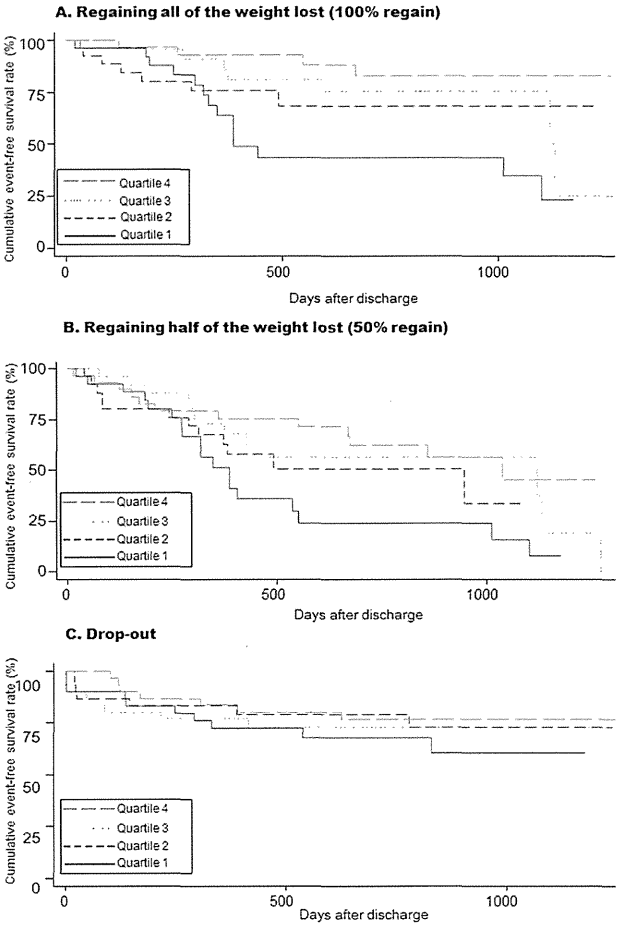

Figure 3 Kaplan–Meier curves for (A) regaining all of the weight lost (100% regain), (B) regaining half of the weight lost (50% regain), and (C) dropout from treatment after discharge in patients with severe obesity stratified by quartiles of achieved weight loss (%) during hospitalization. [Color figure can be viewed in the online issue, which is available at wileyonlinelibrary.com.]

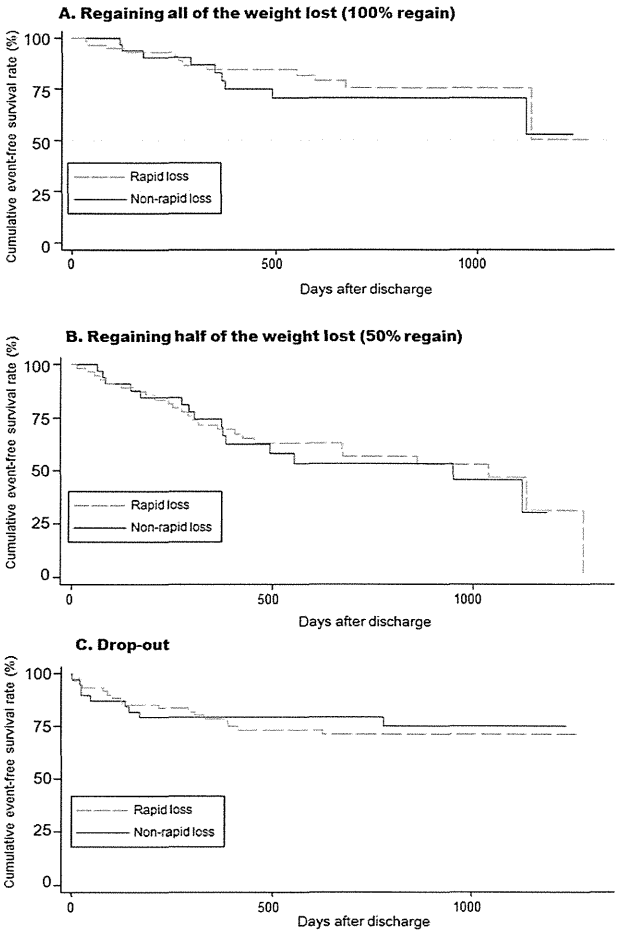

Figure 4 Kaplan–Meier curves for (**A**) regaining all of the weight lost (100% regain), (**B**) regaining half of the weight lost (50% regain), and (**C**) dropout from treatment after discharge in patients with severe obesity stratified by the rapidity of weight loss after admission. [Color figure can be viewed in the online issue, which is available at wileyonlinelibrary.com.]

weight loss and therefore can help them to reach an important therapeutic milestone. In the general population, Linde et al. (21) found that participants who performed daily self-weighing lost significantly more weight than participants weighed themselves weekly, monthly, bi-monthly, or never. However, published evidence about the effect of very frequent weighing (four times per day) has been limited. Although Raynor et al. (22) reported that self-weighing more than once per week was related to a lower BMI, this has not been previously demonstrated for self-weighing more than once daily, as was done in the present study.

Our findings support those reported by several other authors. Nackers et al. (9) showed that initial weight loss was related to adherence and success with a 6-month weight loss program in subjects without diabetes, while Hemmingsson et al. (10) reported that a high baseline BMI and rapid initial weight loss were both independently associated with greater weight loss after 1 year. However, the following differences between our study and these two studies (9,10) should be noted. (a) We employed an inpatient program with comparatively brief hospitalization (mean: 19 days) while the other studies were based on outpatient programs over 6 months. (b) Our patients had more severe obesity (mean: BMI 41.7 kg/m^2) compared with patients in the other studies [mean BMI: 36 kg/m^2 (9) and 30 kg/m^2 (10)].

The present study had several limitations. First, it was performed at a single center and assessed a small patient population, which could limit the generalizability of our findings. Although analyses were adjusted for many covariates that were expected to be confounding factors, the small sample might have resulted in a lack of significant differences in our analyses. Therefore, it will be necessary to perform investigations on a larger scale (including well-designed randomized controlled trials) in the future.

In addition, we used the percent weight loss instead of actual weight loss (in kg) for our analyses. This was done because we considered that evaluation based on actual weight loss is inappropriate when comparing individuals with different constitutions (e.g., losing 3 kg has very different implications for a person who weighs 60 kg compared with a person who weighs 120 kg. Moreover, the effect of weight loss is shown as percentages in the AHA/ACC/TOS Guidelines (5). However, there is still controversy as to whether actual weight loss (in kg) or the percent loss should be evaluated.

In conclusion, when severely obese patients completed a comprehensive inpatient treatment program targeting 5% weight loss, successful weight loss during comparatively brief hospitalization predicted subsequent maintenance of lower weight without increasing the risk of dropout, and rapid weight loss did not increase the risk of subsequent weight gain. Successful in-hospital weight loss might increase the motivation of obese patients. Thus, a short-term intensive inpatient program targeting 5% weight loss can be clinically useful for long-term improvement of weight. However, we could not fully monitor adherence to our program after discharge from the hospital, so further studies will be required to confirm the efficacy of this educational approach. **O**

References

1. WHO.Fact sheet on overweight and obesity [article online]. Available from http://www.who.int/mediacentre/factsheets/fs311/en/. Accessed May 21, 2014.
2. Obesity: preventing and managing the global epidemic. Report of a WHO consultation. *World Health Organ Tech Rep Ser* 2000;894:i-xii, 1-253.
3. American Diabetes Association. Standards of medical care in diabetes–2014. *Diabetes Care* 2014;37 Suppl 1:S14-S80.
4. Berrington de Gonzalez A, Hartge P, et al. Body-mass index and mortality among 1.46 million white adults. *N Engl J Med* 2010;363(23):2211-2219.
5. Jensen MD, Ryan DH, Donato KA, et al. Guidelines (2013) for managing overweight and obesity in Adults. *Obesity* 2014;22(S2):S1-S410.
6. Sasaki A, Wakabayashi G, Yonei Y. Current status of bariatric surgery in Japan and effectiveness in obesity and diabetes. *J Gastroenterol* 2014;49(1):57-63.
7. OECD. OECD Health Statistics 2014, forthcoming, [WWW document]. Available from www.oecd.org/health/healthdata; 2014. Accessed 30 June 2014.
8. Dombrowski S, Knittle K, Avenell A, Araújo-Soares V, Sniehotta F. Long term maintenance of weight loss with non-surgical interventions in obese adults: systematic review and meta-analyses of randomised controlled trials. *BMJ* 2014; 348:g2646.
9. Nackers LM, Ross KM, Perri MG. The association between rate of initial weight loss and long-term success in obesity treatment: does slow and steady win the race? *Int J Behav Med* 2010;17(3):161-167.
10. Hemmingsson E, Johansson K, Eriksson J, Sundström J, Neovius M, Marcus C. Weight loss and dropout during a commercial weight-loss program including a